Measurement of Airborne Particle Concentrations Near the Sunset Crater Volcano, Arizona

Prepared by

Roland R. Benke*
Donald M. Hooper*
James S. Durham*
Donald R. Bannon*
Keith L. Compton†
Marius Necsoiu‡
Ronald N. McGinnis, Jr.‡

Center for Nuclear Waste Regulatory Analyses
Southwest Research Institute®
6220 Culebra Road
San Antonio, Texas 78238-5166
(210) 522-5250
Fax: (210) 522-6081
rbenke@swri.org

September 2007

ABSTRACT

Direct measurements of airborne particle mass concentrations or mass loads are often used to estimate health effects from the inhalation of resuspended contaminated soil. Airborne particle mass concentrations were measured using a personal sampler under a variety of surface-disturbing activities within different depositional environments at both volcanic and nonvolcanic sites near the Sunset Crater volcano in northern Arizona. The level of surface-disturbing activity was found to be the most influential factor affecting the measured airborne particle concentrations, which increased over three orders of magnitude relative to ambient conditions. In addition, as the surface-disturbing activity level increased, the particle size distribution and the majority of airborne particle mass shifted from particles with aerodynamic diameters less than 10 μm [0.00039 in] to particles with aerodynamic diameters greater than 10 μm [0.00039 in]. Above average wind speeds tended to increase airborne particle concentrations under ambient conditions and decrease airborne particle concentrations in the breathing zone above the ground surface during light and heavy surface-disturbing conditions. Overall, the ground surface material type, depositional environment, and percentage of near-surface mass that is resuspendible were not as influential as other factors. A slight increase in the average airborne particle concentration during ambient conditions was found above older nonvolcanic deposits, which tended to be finer grained than the Sunset Crater tephra deposits. An increased airborne particle concentration was realized when walking on an extremely fine-grained deposit, but the sensitivity of airborne particle concentrations to the resuspendible fraction of near-surface grain mass was not conclusive in the field setting when human activities disturb the bulk of near-surface material. Although the limited sample size precluded detailed statistical analysis, the differences in airborne particle

concentration over 900-year weathered volcanic and nonvolcanic deposits appeared to be potentially significant only under heavy surface disturbances.

Key Words: resuspension, airborne particle concentration, redistribution, volcanic ash, mass load

INTRODUCTION

Direct measurements of airborne particle mass concentrations or mass loads are often used to estimate health effects from the inhalation of resuspended contaminated soil (Till and Meyer 1983; Anspaugh et al. 2002). In addition, significant efforts by the scientific community have focused on the respiratory health effects from volcanic ash. Horwell and Baxter (2006) provide a comprehensive review of published clinical, epidemiological, and toxicological studies. As pointed out by Blong (1996), ashfall covers a wide area and, thus, can affect a large number of people relative to other volcanic hazards (e.g., lava flows). Although airborne particle concentrations can reach maximums during heavy ashfall events, eruptions are often short lived. Ashfall deposits, on the other hand, can remain in the local environment for extended periods of time, where they can be resuspended and remobilized, by natural processes or human activities, and contribute to long-term exposure.

The work described in this paper was performed to improve the understanding of natural and human-induced processes at Yucca Mountain, Nevada. Because few data relevant to tephra dispersal, deposition, and subsequent redistribution and resuspension processes are obtainable from existing volcanoes in the Yucca Mountain area, focused field investigations and literature reviews have been conducted for analog sites to evaluate resuspended airborne particle concentrations and mass loads that are representative of basaltic tephra-fall deposits. This field work was conducted to support development of an independent performance assessment review capability and abstracted model that uses an airborne mass load modeling approach (Mohanty et al. 2002; Chapter 6 of Mohanty et al. 2005; Benke et al. 2006). Whereas the previous health-related studies have focused on cristobalite (crystalline form of SiO_2) in airborne particle concentrations from silicic eruptions due to a potential for carcinogenic or fibrotic respiratory health effects, tephra from basaltic volcanism in the Yucca Mountain region

lacks a crystalline silica phase. In addition to potentially different respiratory health implications, silicic (e.g., Mount St. Helens, Washington) and basaltic tephra deposits can exhibit dissimilar average grain sizes, particle shapes, and environmental aging effects. This work, therefore, was focused on basaltic eruptions, including airborne particle measurements over basaltic tephra deposits.

Field measurements have been reported previously for Cerro Negro tephra-fall deposits in Nicaragua, another basaltic volcano considered to be a potential analog for an eruption in the vicinity of Yucca Mountain (Hill et al. 2000). Measurements were taken four years after the 1995 eruption above the tephra deposits located about 5 km [3.1 mi] from the vent. Digging and driving over deposits resulted in airborne mass loads on the order of ~10 mg m^{-3}. Walking over deposits resulted in airborne mass loads on the order of ~1 mg m^{-3}. Airborne mass loads over undisturbed deposits were on the order of ~0.1 mg m^{-3} in 4 ± 2 m s^{-1} [9 ± 4 mi h^{-1}] winds. Similar ranges of airborne particle concentrations were measured by Searl et al. (2002), who evaluated potential risks to the respiratory tract of exposed populations arising from inhalation of silicic volcanic ash ejected from the Soufrière Hills Volcano on the island of Montserrat. Horwell and Baxter (2006) provide a review of respiratory health studies for volcanic ash. These reports primarily describe measured airborne particle concentrations or mass loads from relatively recent silicic volcanic eruptions.

Located in a semiarid climate of northern Arizona in the Desert Southwest, Sunset Crater is a suitable analog for potential volcanic processes and posteruption surface processes at Yucca Mountain, Nevada, because of comparable styles of volcanism, type of eruptive products, and climate. Sunset Crater is a 900-year-old basaltic scoria cone volcano with a surrounding deposit of tephra ejected from a violent Strombolian-type eruption (Amos 1986). Eruptive activity at Sunset Crater began in 1064 or 1065 A.D. (Smiley 1958) and continued, probably intermittently, for about 150 years (Holm and Moore 1987; Tanaka et al. 1990). The

plateau on which the San Francisco Volcanic Field is situated has an average elevation of about 2,150 m [7,000 ft]. The mean annual precipitation at this elevation is approximately 500 mm [20 in], and temperatures are characteristic of high-altitude climates (Sellers and Hill 1974). From early July until early September, afternoon thunderstorms develop almost daily over the higher terrains. These short-lived convective storms provide approximately half the annual precipitation for the region and are triggered by moisture from the Gulf of Mexico. Additional precipitation is provided by winter storms that enter the state from the west with moisture from the Pacific Ocean. About 75 percent of this precipitation falls as snow (Sellers and Hill 1974). Elevations at the specific measurement sites, which included measurements on the plateau and lower terrains, ranged from 1,420 m [4,660 ft] to 1,950 m [6,400 ft]. The vegetative cover is comparable to the Yucca Mountain region, with an annual precipitation of approximately 150 mm [6 in], at the nonvolcanic sites in the northeast, but vegetative cover is more widespread at the higher elevation volcanic sites near Sunset Crater. Because vegetation affects the shear velocity profile near the ground surface and restricts the airborne particle flux (Wiggs 1997), airborne particle concentrations from resuspension are generally expected to be lower in areas with greater vegetative cover.

Field measurements were performed over a range of surface-disturbing conditions so that measurement results could be easily related to modeling of human activities that are representative of the characteristics of the receptor. Because particle size is an important factor for determining deposition within the respiratory tract and estimating health effects, the field measurements also obtained information on the airborne particle size distribution in addition to the total mass concentration of airborne particulates. In addition to providing airborne resuspension information for various ground surface material types, depositional environments, and levels of surface-disturbing activities, field investigations on the 900-year-old tephra deposit

from Sunset Crater provide insights on the long-term behavior and persistence of airborne particle concentrations following a volcanic eruption.

MATERIALS AND METHODS

Airborne particle measurements were acquired over both volcanic (Sunset Crater tephra) and nonvolcanic ground surface material. To more directly apply insights gained from field work to system-level models, field sites were selected to be representative of two general material types (volcanic versus nonvolcanic) and three depositional environments (primarily non-reworked deposits, redistributed fluvial deposits, and redistributed eolian deposits). Simplified, nontraditional types and depositional environments of ground surface material are used in this paper. Much of the surface material in the Sunset Crater region is of volcanic origin. However, the volcanic sites in this study specifically refer to regions covered by 900-year-old basaltic tephra from the Sunset Crater eruption. In addition, "primarily non-reworked" does not imply age or degree of weathering but rather that deposits are not in an active region of fluvial or eolian erosion and redistribution. At each site, separate airborne particle measurements were performed for three different levels of surface-disturbing activity:

- Ambient measurements without human surface-disturbing activity
- Light disturbance measurements associated with walking or setting up equipment
- Heavy disturbance measurements associated with digging, hoeing, or collecting surface samples

Based on combinations of ground surface material type, depositional environment, and surface-disturbing conditions, there are 18 classes of airborne particle concentration measurements (Table 1). Each airborne particle measurement corresponds to one of the 18 measurement classes. Fig. 1 displays a map of the region and identifies the location of the measurement sites.

Airborne particle measurements were acquired during the daytime. Ambient measurements used a tripod to position the sampler inlet at a height of 1.5 m [4.9 ft] above the ground surface. For the light and heavy disturbance measurements, the sampler was worn on an upper chest harness or on the waist by the individual performing the surface-disturbing activity. As time permitted, multiple measurements at the same site were performed on different days to provide information about variability in the field. In addition to airborne particle measurements, surface samples were collected at each site to a depth of about 1 cm [0.4 in] using an inscribed template and flat trowel. Fig. 2 shows the radial sampling grid, which was centered at the location of the ambient airborne particle measurement. Surface sampling was not performed during the ambient airborne particle measurement. The sampling depth of 1 cm [0.4 in] was selected to be both practical (surface roughness effects precluded straightforward sampling of thinner, millimeter-thick layers) and representative of the material available for resuspension with and without human-induced surface-disturbing activities. Surface samples were sieved in the laboratory to yield grain size distributions for comparison to the total and particle-size-dependent airborne particle concentrations.

Two sites were selected for primarily non-reworked, nonvolcanic material (N-Ps and N-Pa). Site N-Pa was unique in that its ground surface consisted of alluvium, exposed from previous excavation activities that removed overlying layers of tephra. The detail window of Fig. 1 for Site N-Pa shows that the underlying nonvolcanic alluvium is exposed only in a small area, surrounded by tephra-covered areas. Although measurements at Site N-Pa may infer what airborne particle concentrations would have been prior to the Sunset Crater volcanic eruption, the influence of the surrounding tephra and previous human excavation activities have not been quantified by this work. In contrast, Site N-Ps consisted of an area of weathered, but primarily non-reworked, sandstone. Airborne particle measurements were taken at both sites for comparison purposes. None of the measurement sites were characterized as having a desert

pavement. Desert pavement is characteristic of the inactive alluvial surface of the Yucca Mountain region, where fine particles infiltrate below the upper surface layers of coarser particles to create a surface with a decreased susceptibility to airborne resuspension. Thus, the nonvolcanic sites investigated with primarily non-reworked depositional environments may be associated with higher airborne particle concentrations, compared to undisturbed desert soils with pavements, and may not be good analogs for inactive surfaces of the Yucca Mountain region.

Wind speed measurements were not acquired at the field sites. The wind speed data from the Flagstaff Pulliam Airport are presented in Tables 2, 3, and 4 to provide a general indication of average winds in the region on the day that airborne particle measurements were taken.

Each airborne particle measurement was performed with a personal airborne particle sampler and portable air pump. A single type of particle sampler (RESPICON™ Particle Sampler, Model 8522, TSI Incorporated, Shoreview, MN 55126-3996) was used with one of two types of pumps (Model Air Pro 6000D Listed 87Y4, Bios International Corporation, Butler, NJ 07405; Model Libra Plus LP-7, A.P. Buck Inc., Orlando, FL 32809, only used for long sampling times for some of the ambient measurements). In addition to measuring the total suspended particle concentration, information on airborne particle size also was obtained. The RESPICON™ particle sampler (hereafter referred to as RespiCon) is a multistage virtual impactor, where sampled particles are separated by size with diverted air flows within the device and preferentially collected on one of three filters according to their aerodynamic diameter. The sampling efficiency is complex and described by particle-size-dependent curves (TSI Incorporated 2006). Partitioning of air flow and deposition within the device stages was designed to mimic deposition in different regions of the human respiratory tract, and 50-percent cut sizes are used to characterize the sampled particle size ranges associated with each filter. In general terms,

each sampler measurement resulted in separate measurements for particles with aerodynamic diameters less than 4 µm [0.00016 in], between 4 and 10 µm [between 0.00016 and 0.00039 in], and greater than 10 µm [0.00039 in]. The total airborne particle concentration was determined by summing the particle mass collected on all three filters. The presented concentrations are equivalent to airborne mass loads of resuspendible particles or airborne particle mass concentrations. The shortened term “particle concentration” is used for simplicity in this paper and does not imply particle counting (i.e., number per unit volume of air).
A summary of the literature on the RespiCon sampler is provided in this paper.

RespiCon samplers have been used to measure airborne particle concentrations of naturally occurring radioactive material from pipe scale rattling and cleaning in the petroleum industry (Hamilton et al. 2004). RespiCon samplers have also been used to measure airborne particle concentrations in an indoor workplace (e.g., Tatum et al. 2002; Rando et al. 2005) and laboratory environments (Li et al. 2000; Feather and Chen 2003). In contrast to other instruments that were highly affected by wind direction and reported measured concentrations that could vary by factors of 2 to 10 (Li et al. 2000), the RespiCon sampler was not sensitive to wind direction, due to its 360-degree inlet, and is therefore appropriate for outdoor measurements. When the RespiCon was compared to reference samplers, Rando et al. (2005) indicated that there was no significant difference between sampling in the free-field versus simulated on-body setups. This result indicates that the RespiCon is also well suited for ambient measurements, where a tripod was used to position the sample at breathing zone height of 1.5 m [4.9 ft], and allows meaningful comparisons with the light and heavy disturbance measurements, where the sampler was worn by the field investigator disturbing the ground surface.

Performance of the RespiCon sampler and the need for applying a correction factor to the RespiCon measurements have been discussed in the literature. Tatum et al. (2002) found

the RespiCon results closely corresponded to results from other instruments and reported that microscope analysis of RespiCon filters was consistent with expected performance characteristics. Following the Li et al. (2000) work, the RespiCon manufacturer recommended that users discontinue application of the previous multiplicative correction factor of 1.5 to the mass of the third stage sample for matching the German standard for total dust (TSI Incorporated 2001). Indoor measurements by Rando et al. (2005) without the correction factor of 1.5 indicated that the RespiCon undersampled inhalable dust by an average of 25 percent and overestimated thoracic dust by 48 percent. In calm air, settling chamber measurements, Feather and Chen (2003) reported undersampling of particles with aerodynamic diameters greater than 10 μm [0.00039 in]. Considering the wind tunnel measurements of Li et al. (2000), Feather and Chen suggested that a correction factor may be needed for the RespiCon in calm air environments, but that the sampler may perform reasonably well without a correction factor in moving air environments. Li et al. (2000) performed RespiCon sampler measurements, without the correction factor of 1.5, in a wind tunnel at 0.55 m s^{-1} [1.2 mi h^{-1}] and 1.1 m s^{-1} [2.5 mi h^{-1}] to be representative of moderate to high workplace wind speeds. At the lower wind speed, the measured efficiencies of the RespiCon sampler matched the respirable, thoraric, and inhalable conventions by American Conference of Governmental Industrial Hygienists (1995) to within 10 percent for various particle sizes. At the higher wind speed {1.1 m s^{-1} [2.5 mi h^{-1}]}, the largest particles {68 μm [0.0027 in] aerodynamic diameter} were oversampled by 25 percent, which resulted in a noted deviation from the inhalable convention. The measurements presented in this paper were performed outdoors in winds with average daily speeds that ranged from 1.7 to 7.6 m s^{-1} [3.8 to 17 mi h^{-1}], which could imply an increased potential for oversampling large airborne particles {aerodynamic diameters greater than 10 μm [0.00039 in]}. Based on both manufacturer recommendations (TSI Incorporated 2001) and review of the literature, regarding potential oversampling of large particles in higher outdoor

winds, no correction factors were used in this work. Overall, the reported differences in studies reported in the literature ranged up to tens of percent and are not expected to be the dominant source of uncertainty, considering the much larger amount of expected variability in the outdoor measurements from resuspension activities during continuously changing atmospheric conditions.

Premeasurement flow rates were checked using a calibrated flowmeter (Bios International Corp., DryCal DC-Lite Model DCL-M Rev. 1.11). Measurements of the atmospheric pressure (Digiquartz Portable Standard, Model 740-45A, Paroscientific Inc., Redmond, WA 98052) and temperature (Humidity and Temperature Meter Model HM34C, Vaisala, Helsinki, Finland) were used to convert flow rates measured in the field to flow rates at standard temperature and pressure for comparison to the manufacturer-recommended ranges of operation.

Filters were processed before and after sampling according to the following procedure. The filters were dried in an oven (Stabil-Therm, Model OV-510A-3, BlueM, New Columbia, PA 17856-9396) for 2 hours at approximately 50 °C [120 °F] and allowed to cool to room temperature for 2 hours while covered. After drying, filters were weighed on a calibrated microbalance (Model XP205DR, Mettler-Toledo Inc., Columbus, OH 43240). Prior to weighing filters on the microbalance, each filter was placed on a Polonium source (Model 2U500, NRD LLC, Grand Island, NY 14072-0310) for 30 seconds to remove static charges. Each filter was weighed twice, and the two weights were compared. For those filters with weight differences of less than 0.05 mg (i.e., two standard deviations from a repeatability study for the microbalance), an average weight was calculated from the two separate weighings. For those filters with weight differences of at least 0.05 mg, a third weighing was performed. The third weight was paired with the closest one of the first two weights to determine the average filter weight. In a couple of instances, the third filter weight was equally close to each of prior two weights.

In those cases, the third measurement also equaled the average of the first two measurements, which was assigned as the average filter weight.

Pre- and postsampling filter weights, air pump flow rates, and sampling times were used to calculate the airborne particle mass concentration. The calculation of measurement uncertainty for airborne particle concentrations required additional information on uncertainties of measured filter weights and flow rates. Uncertainties were propagated into the calculations of the total and size-dependent airborne particle concentrations. Detailed equations for airborne particle concentration and its measurement uncertainty are presented in the Appendix. The calculated measurement uncertainties are not intended to quantify the variability of field and human surface-disturbing conditions, which is addressed in the Discussion section.

RESULTS

Results of the airborne particle measurements are presented for increasing levels of surface-disturbing activity. In addition to the airborne particle measurements, grain size information and images from the surface samples are displayed.

For ambient conditions (i.e., no surface-disturbing human activity), total airborne particle concentrations are presented in Table 2 and Fig. 3(a). Fig. 3(b) displays the particle size distribution as fractions of the measured total particle concentration. Ambient measurements were acquired for sampling durations of 7 to 10 hours, except for the two measurements with large uncertainty bars in Fig. 3(a) that resulted from a shorter sampling duration of 2 hours.

For light disturbance conditions, total airborne particle concentrations are presented in Table 3 and Fig. 4(a). Fig. 4(b) displays the particle size distribution as fractions of the measured total particle concentration during light disturbance activities. Measurements during continuous light surface-disturbing activities were acquired for sampling durations of 43 to 90 minutes. In addition, an airborne particle measurement while walking was collected at the extra fluvial site where the unpaved forest route road crossed Deadman Wash, northwest of Sunset

Crater (Site Extra-F in Fig. 1). Results for Site Extra-F are not grouped with the results from the other sites and are presented separately (refer to Discussion section). The total airborne particle concentration while walking for 45 minutes on the fine-grained fluvial deposit at Site Extra-F was 11.1 ± 0.4 mg m^{-3} during average daily winds of 4.65 m s^{-1} [10.4 mi h^{-1}]. For Site Extra-F, airborne particles with aerodynamic diameters less than 4 μm [0.00016 in], between 4 and 10 μm [between 0.00016 and 0.00039 in], and greater than 10 μm [0.00039 in] accounted for about 4 ± 2, 33 ± 2, and 64 ± 2 percent of the total airborne particle concentration.

For heavy disturbance conditions, total airborne particle concentrations are presented in Table 4 and Fig. 5(a). Fig. 5(b) displays the particle size distribution as fractions of the measured total particle concentration during heavy disturbance activities. Measurements during continuous heavy surface-disturbing activities were acquired for sampling durations of 30 to 50 minutes. Note that target sampling durations were selected prior to performing the measurements and analyzing the results so that enough particulate matter would be deposited on the filters to result in acceptable measurement uncertainties for the airborne particle concentrations. The sampling durations used for the presented measurements, therefore, provide no indication of a fraction of time individuals would spend outdoors engaged in activities that generate significant amounts of dust. For example, anticipated time spent by individuals in each surface-disturbance category during the course of a year is beyond the scope of this paper.

Figs. 6 and 7 present images taken in the laboratory of the surface samples from the volcanic and nonvolcanic sites. An image of the fine-grained deposit at Site Extra-F is displayed in Fig. 8. Grain-size distributions from the volcanic and nonvolcanic sites are plotted in Figs. 9 and 10 from sieved surface samples. Geological composition descriptions and the fraction of resuspendible particles are provided for context in Table 5.

DISCUSSION

A discussion is provided on the airborne particle measurements for increasing levels of surface-disturbing activity. The discussion also addresses the grain size evaluation of the surface samples, the influence of depositional environment, and comparison to other work.

Although the term “significant” is used freely throughout this paper, statistical tests on the measurement data were not performed due to the limited sample size. Use of significance terminology does not imply statistical significance. Herein, significance relates to the influence some aspect appeared to have on the measured results in light of uncertainty and variability in the field measurements. Targets for sampling durations were selected prior to performing the measurements and were based on estimates of measurement uncertainties with the intent that actual standard durations, relative to the measured concentration, would be no more than a few tens of percent. The sampling durations do not represent the fraction of time individuals might spend generating dust outdoors. In a few cases, pump battery lifetimes resulted in shorter sampling durations.

Ambient Conditions

Overall, the total airborne particle concentration ranged from 0.1 to 0.4 mg m^{-3}. On different measurement days at the same site, the total airborne particle concentration varied by about a factor of 2. For ambient conditions, airborne particle concentration over 900-year weathered volcanic and nonvolcanic deposits appear comparable within the limits of the measurement uncertainty and variability. Higher wind speeds during measurements on different days at the same site tended to result in greater total airborne particle concentrations. From Fig. 3(b), most of the airborne mass was associated with particles with aerodynamic diameters less than 10 μm [0.00039 in]. Airborne particles with aerodynamic diameters less than 4 μm [0.00016 in], between 4 and 10 μm [between 0.00016 and 0.00039 in], and greater than 10 μm [0.00039 in] accounted for about 45, 40, and 15 percent of the total airborne particle

concentration on average with respective ranges of approximately 25–55, 20–50, and less than 40 percent.

Some of the airborne particle sampling measurements were performed coincident with forest fires in the region, which had the potential to increase ambient airborne particle concentrations. The most significant fire occurred during the later part of the field campaign in the Oak Creek Canyon area located approximately 48 km [30 mi] southwest to west-southwest of the Sunset Crater measurement sites. During several of the sampling days, the predominant wind direction was from the west to southwest, which blew smoke plumes generally toward the measurement locations. During the airborne measurements, however, the smell of smoke was not present. Nevertheless, the potential for the forest fires to elevate the measured total airborne particle concentration was investigated for ambient conditions because these measurements were expected to be the most affected, if at all, as the light and heavy measurements were influenced by the local surface-disturbing activities. Separate measurements of the total airborne particle concentration were compared for the same site under ambient conditions, where one measurement taken before the fire was compared to another measurement taken during the forest fire. In all three cases, the ambient concentrations measured during the forest fire were lower (by more than 1 or 2 standard deviations) than ambient measurements acquired before the forest fire. For two of the three cases, winds during the fire directed the smoke toward the measurement location. Based on the comparisons, it appears that the distant forest fire did not elevate the measured total airborne particle concentrations. During ambient measurements coincident with the forest fire, an increase in airborne particle concentrations associated with small particles also was not evident in either a relative or absolute sense.

Light Disturbance

Light disturbance measurements primarily involved continuous walking on the deposits

and were characterized by leaving footprints at times and intermittently generating small amounts of visible airborne dust near the ground surface to about ankle height. Total airborne particle concentrations during light surface-disturbing activities are presented in Table 3 and Fig. 4(a). Except for fluvial deposits, the total airborne particle concentration ranged from about 0.5 (about 0.2 if the lowest result is included) to 2 mg m^{-3}. For fluvial deposits, the range appeared to be expanded at the higher end, with total airborne particle concentrations ranging from up to 5 mg m^{-3}. The lowest result of 0.15 mg m^{-3} from the second measurement in Table 3 may not be appropriate to define the lower end of the overall range, because a slight loss of mass, within one standard deviation of the measurement uncertainty, was recorded for two of the three filters and biased the measured total and particle-size-dependent airborne particle concentrations. The presented low concentration corresponds to the mass gained on the single filter for the smallest particle sizes and the total sampled volume of air from all three stages with no contributions from the other two filters for the larger particle sizes. Allowing negative mass contributions from the filter weight measurements, which indicated a loss of mass for two of the three filters, would have resulted in nonphysical negative particle-size-dependent concentrations. The indicated loss of mass is believed to be caused by measurement uncertainty in filter weighing (see Appendix). Based on the other measurement results for particle-size-dependent concentrations, none were dominated solely by the smallest particles {aerodynamic diameters less than 4 μm [0.00016 in]}. For these reasons, particle size information was not presented for this measurement in Fig. 4(b).

On different measurement days at the same site for similar disturbance levels, the total airborne particle concentration during light disturbance activity varied by factors between less than 2 to about 5. The additional resuspension variability associated with the human-induced light surface disturbance activity is the likely cause for the increase in overall variability for light disturbance measurements relative to ambient conditions. For light disturbance conditions, the

differences in airborne particle concentration over 900-year weathered volcanic and nonvolcanic deposits do not appear to be significant given the variability in measurement activities and resuspension. When wind speeds were significantly higher during measurements on different days at the same site, increased winds tended to blow airborne particulates away more quickly from the field investigator, who was generating the dust and wearing the airborne particle sampler, and decreased the measured total airborne particle concentration.

Fig. 4(b) displays the particle size distribution as fractions of the measured total particle concentration. Overall, about half of the airborne mass was associated with particles with aerodynamic diameters greater than 10 μm [0.00039 in].

Walking on the fine-grained deposit at the extra fluvial site (Extra-F), however, produced much larger, visible dust clouds that sometimes extended into the breathing zone. The results of this site measurement were not grouped with the results for the other sites. The extra fluvial site (Extra-F) was selected specifically because it consisted of the finest-grained surface material encountered during the field campaign (refer to Table 5 for further description). In contrast to the other sites, measurement of this localized fluvial deposit is not intended to be representative of the larger fluvial system and was acquired to investigate how a substantial shift in the grain-size distribution affected the measured airborne particle concentration.

Heavy Disturbance

Total airborne particle concentrations during heavy surface-disturbing activities are presented in Table 4 and Fig. 5(a). For volcanic deposits, the total airborne particle concentration ranged from about 2 to 100 mg m^{-3} during continuous heavy surface-disturbing activity. For nonvolcanic deposits, the total airborne particle concentration ranged from about 2 to 10 mg m^{-3} during continuous heavy surface-disturbing activity. Based on the measurements performed, heavy surface-disturbing activity over 900-year weathered volcanic deposits was found in two instances to produce higher total airborne particle concentrations

than over nonvolcanic deposits, thereby expanding the overall range of concentrations for volcanic deposits at its upper end. The upper end of these ranges represents vigorous activity to bound the short-term airborne particle concentration. The sustained, vigorous digging activities, which resulted in total airborne particle concentrations of about 10 to 100 mg m^{-3}, were performed on days with below-average to average wind speeds for that month (Table 4) and were characterized by observers as generating visible clouds of dust that extended into the breathing zone. Although the personal sampler was worn in an upper chest harness or on the waist, some portion of digging and surface sampling activities included kneeling, which places the sampler and breathing zone closer to the ground surface where airborne particle concentrations are expected to be greater than for more upright activities such as hoeing.

On different measurement days at the same site for similar disturbance levels, the total airborne particle concentration during heavy disturbance activity varied by factors between 5 to 50. Relative to light disturbance and ambient measurements, the greatest amount of overall variability was associated with the heavy disturbance measurements. As the surface-disturbing activities increased to heavy levels, the type of activity performed (i.e., hoeing, surface sampling, and digging) and effect from different field investigators resulted in a larger range of airborne particle concentrations, compared to the range obtained from the light disturbance measurements. When wind speeds were higher during measurements on different days at the same site, increased winds tended to blow airborne particulates away more quickly from the field investigator, who was generating the dust and wearing the airborne particle sampler, and decreased the measured total airborne particle concentration. For the smallest increase in wind speed (of 30 percent) during measurements on different days at the same site for similar heavy disturbance levels, the airborne particle concentration was not reduced and, in fact, was significantly higher (10.4 mg m^{-3} versus 2.2 mg m^{-3}), which implies that actions of each field investigator and specifics of each measurement are especially significant under heavy

disturbance conditions. In this case, different investigators performed digging and hoeing at the same site on different days. Probable causes for the different results include differences in the amount of energy expended by each field investigator and transferred to the ground surface, and differences in the location of the disturbing activity on the ground surface relative to the local wind direction (e.g., sampler downwind, crosswind, or upwind of the point of resuspension).

Fig. 5(b) displays the particle size distribution as fractions of the measured total particle concentration. For volcanic deposits, a majority of the airborne mass was associated with particles with aerodynamic diameters greater than 10 μm [0.00039 in]. For volcanic deposits, airborne particles with aerodynamic diameters less than 4 μm [0.00016 in], between 4 and 10 μm [between 0.00016 and 0.00039 in], and greater than 10 μm [0.00039 in] accounted for about 10, 30, and 60 percent of the total airborne particle concentration on average with respective ranges of approximately 3–15, 20–40, and 50–70 percent. For nonvolcanic deposits, Fig. 5(b) shows that a greater percentage of the airborne mass was associated with fine particles. For nonvolcanic deposits, airborne particles with aerodynamic diameters less than 4 μm [0.00016 in], between 4 and 10 μm [between 0.00016 and 0.00039 in], and greater than 10 μm [0.00039 in] accounted for between 20–35 percent, between 20–35 percent (10 percent for the fluvial nonvolcanic deposit), and about 45 percent (65 percent for the fluvial nonvolcanic deposit) of the total airborne particle concentration. For the heavy disturbance results, higher total airborne particle concentrations were generally correlated with increased concentrations of larger particles {aerodynamic diameters greater than 10 μm [0.00039 in]}, which accounted for approximately 50–70 percent of the total airborne particle concentration.

Grain-Size Evaluation

Grain-size distributions from sieving samples in the laboratory are displayed in Figs. 9 and 10 for the volcanic and nonvolcanic sites. The grain-size information was distilled into a

single metric for each sample in Table 5, namely the percent of surface sample mass with physical grain diameters less than 106 μm [0.00417 in]. This grain size agrees well with the size of suspended particles having diameters less than 100 μm [0.00394 in] (Anspaugh et al. 1975). The 106-μm [0.00417-in] size was chosen to represent the largest particle size likely to contribute to the airborne particle concentration at the breathing zone following resuspension from the ground surface. The 106-μm [0.00417-in] physical diameter is also close to the 100-μm [0.00394-in] aerodynamic diameter that defines the upper range of particle sizes for inhalability by the American Conference of Governmental Industrial Hygienists (1995) and the largest particles modeled for deposition in the human respiratory tract by the International Commission on Radiological Protection (1994).

Surface samples from Site V-P provide some indication of the initial grain size of the Sunset Crater tephra deposit, which is fairly coarse. In volcanological terms, the deposit is composed of coarse ash, lapilli, and small volcanic blocks and bombs. Compared to Site V-P, the fluvial and eolian deposits of Sunset Crater tephra at Sites V-F and V-E were generally finer grained, because redistribution tends to sort the material by selectively transporting grains of a certain size range. The eolian deposits are the most sorted (i.e., having a narrow grain-size distribution) with the finest grains winnowed out and removed from the eolian deposit; coarser grains were left behind as a lag deposit (Table 5).

Samples from the nonvolcanic sites are older and have undergone chemical and mechanical degradation and weathering with a median grain size that is finer compared to the Sunset Crater tephra samples (except for the sandstone at Site N-Ps, which provided a very thin layer of loose surface material for sampling). These older materials also contain more dust or an accumulated eolian component, which is typical of semi-arid to arid regions. Overall, greater fractions of near-surface sample mass are available for airborne resuspension at the nonvolcanic sites (Table 5). Even though regional wind speeds were generally lower during the

ambient measurements at the nonvolcanic sites (Table 2), an average airborne particle concentration of 0.28 ± 0.03 mg m^{-3} was obtained at the nonvolcanic sites, which exceeded the average airborne particle concentration of 0.19 ± 0.03 mg m^{-3} at the volcanic sites. Increased amounts of resuspendible material is a likely reason for the general increase in airborne particle concentration at the nonvolcanic sites during ambient conditions. During light and heavy surface disturbances, an overall increase in airborne particle concentration above the nonvolcanic deposits was not found. Although a slight increase in airborne particle concentration can be attributed to grain size effects for the ambient measurements, the grain size of the surface layer was not found to be a significant factor in determining the airborne particle concentration during human-induced surface disturbances. Other factors were more important, such as surface-disturbing activity level. The extremely fine-grained deposit at the extra fluvial site, however, proved to be one notable exception. This material contained a large fraction of resuspendible and inhalable material (62 percent of grain mass less than 106 μm [0.00417 in] compared to the range of 0.6–27 percent for the other sites in Table 5). The total airborne particle concentration was approximately a factor of 6 higher than the average value for light disturbance at the other sites. Particles with diameters greater than 0.3 mm [0.01 in] represent about 10 percent of the near-surface mass of the Extra-F deposit (Fig. 10). The combination of a very large fraction of resuspendable particles and the lack of contiguous coarse grain structure to stabilize the deposit during its disturbance is believed to result in the increased susceptibility of the Extra-F deposit to airborne resuspension. This comparison during light disturbances indicates that grain size can be a significant factor in determining the airborne particle concentration, but appreciable differences in grain size are needed to surpass

other factors, such as human-induced resuspension variability, for the effect to be realized in a field setting when human activities disturb the bulk of near-surface material.

Influence of Depositional Environment

In addition to comparisons between volcanic and nonvolcanic material, the influence of depositional environment (i.e., primarily non-reworked, reworked fluvial, and reworked eolian) was also assessed. Influences due to the depositional environment cannot be differentiated from grain size effects with the present set of measurements. Grain-size information for each depositional environment was compared for the same material (volcanic or nonvolcanic) in this subsection. In general, fluvial deposits were finer grained but not substantially finer grained than the other deposits. For volcanic sites, the highest percentages for grain mass with diameters less than 106 μm [0.00417 in] were 3 percent for fluvial channel deposits and 2 percent for eolian deposits. For nonvolcanic sites, the highest percentage was 27 percent for fluvial deposits, followed by 20 percent for the primarily non-reworked deposit of alluvium. Other factors such as differences in geochemistry, surface layer structure, surface roughness, surface deposit density, particle density, particle shape, and surrounding vegetative cover were not investigated. It can be surmised that grain size may be partly responsible for the implied increase in susceptibility of fluvial deposits to airborne resuspension. Additional investigations are needed to draw more definitive conclusions.

As pointed out for the light disturbance measurements, a couple of measurements over fluvial deposits expanded the observed range to higher airborne concentrations. Although this specific trend was not apparent under ambient and heavy disturbance conditions, measurements over fluvial deposits recorded the highest and third highest concentrations in both cases. Because subtle differences are masked by variability in the resuspension measurements, the implied increase in susceptibility of fluvial deposits to airborne resuspension is far from conclusive.

Comparison to Other Work

Total airborne particle concentrations measured at Sunset Crater under ambient conditions (0.1–0.4 mg m^{-3}) were slightly higher than ambient concentrations (~0.1 mg m^{-3}) measured with the same instruments at Cerro Negro, Nicaragua, over a relatively fresh, 4-year-old basaltic tephra deposit in directly measured surface winds of 4 ± 2 m s^{-1} [9 ± 4 mi h^{-1}] (Hill et al. 2000). Wind speeds during ambient measurements were comparable for the two field campaigns. In general, ambient airborne particle concentrations might be expected to be higher over a younger tephra deposit. The annual rainfall for the Cerro Negro region is approximately 1 m [40 in]. In addition, the region received roughly 2 m [80 in] of rainfall from Hurricane Mitch about six months prior to the Cerro Negro measurements in Hill et al. (2000). The relatively lower concentrations at Cerro Negro may be due to the down washing of fine particles into the deposit during periods of high rainfall rates.

Moore et al. (2002) reported airborne PM_{10} concentrations, with aerodynamic diameters less than 10 µm [0.00039 in], from the Soufrière Hills volcano on the island of Montserrat, where the type of tephra (andesite and dacite) tends to be finer grained than the basaltic tephra at Sunset Crater. Twenty-four-hour-average PM_{10} concentrations from resuspension (i.e., not during ashfall events) ranged from less than 0.1 to 0.3 mg m^{-3} for ambient conditions at static monitoring sites. Higher concentrations from resuspension were recorded for a single site near a main road with significant human activity. Compared to daily PM_{10} concentrations during ashfall events, daily resuspension PM_{10} concentrations could reach ashfall levels but were generally lower over longer time periods. PM_{10} concentrations would have to be scaled up to allow comparisons to our measurements of total airborne particle concentration. Alternatively, the fraction of the total concentration for particles with an aerodynamic diameter less than 10 µm [0.00039 in] can be used to convert the short-term Sunset Crater measurements to equivalent short-term PM_{10} concentrations. Since the airborne mass during ambient conditions

at Sunset Crater mainly consisted (about 85 percent on average) of particles with an aerodynamic diameter less than 10 μm [0.00039 in], equivalent PM_{10} concentrations at Sunset Crater would be less than 0.1 to 0.3 mg m^{-3}, which agree well with the daily PM_{10} concentration ranges observed at Montserrat for fresh ash deposits.

Searl et al. (2002) measured personal exposure to silicic ash from the Soufrière Hills volcano and reported airborne PM_{10} concentrations, averaged over 4- to 8-hour shifts, that ranged from 0.4 to more than 20 mg m^{-3} for outdoor activities during June 1997. PM_{10} concentrations were approximately 10–20 mg m^{-3} for mowing grass outside and sweeping inside. Reduced personal exposure concentrations (mean PM_{10} concentrations of about 0.1 mg m^{-3} for outdoor occupations) were measured in 2000 following rainstorms during the autumn of 1999 that removed much of the remaining loose ash from occupied areas. Other personal exposure measurements during outdoor activities on silicic ash deposits have been performed for the Soufrière Hills volcano (Horwell et al. 2003) and Mount St. Helens {e.g., Buist et al. (1983) measured daytime total suspended particulate concentrations between 0.8 and 2.3 mg m^{-3} in the breathing zone for children at a summer camp where about 1.2 cm [0.5 in] of ash was deposited from the June 12, 1980, eruption of Mount St. Helens}, but are not discussed further in this paper because of the differences in silicic and basaltic tephra deposits.

As part of its established monitoring program, the Arizona Department of Environmental Quality performed airborne particulate monitoring of PM_{10} concentrations at 10 sites around Phoenix, Arizona (http://www.azdeq.gov/function/forms/archives.html accessed on February 23, 2007). Continuous daily measurements of airborne particulates are not collected in northern Arizona, but some infrequent 24-hour measurements (e.g., every sixth day) are gathered for annual summary purposes. Even though the airborne particle concentrations are expected to be greater in the Phoenix area, those comprehensive data were investigated for insights. During the month in which this field campaign was conducted, daily 24-hour-averaged PM_{10}

concentrations were often less than 0.1 mg m^{-3} (reported concentrations at all 10 monitoring sites were less than 0.1 mg m^{-3} on 17 out of 30 days). On 7 out of 30 days, 24-hour-averaged PM_{10} concentrations for at least one monitoring site exceeded 0.15 mg m^{-3}, which is the value of the National Ambient Air Quality Standard for 24-hour PM_{10} concentration set by the U.S. Environmental Protection Agency. The two highest daily 24-hour-averaged PM_{10} concentrations of 0.47 mg m^{-3} and 0.43 mg m^{-3} were recorded on consecutive days at different monitoring sites later in the month. While winds gusted up to 14 m s^{-1} (32 mi h^{-1}) and up to 18 m s^{-1} (40 mi h^{-1}) on two days earlier in the month, hourly PM_{10} concentrations of 0.53 mg m^{-3} and 0.66 mg m^{-3} were reported at two different monitoring sites. At each of those two sites on the same day as the high hourly concentration, the 24-hour-averaged PM_{10} concentration was 0.16 mg m^{-3}, which was lower than the high hourly value by a factor of about 3 or 4. Unfortunately, these measurements do not allow for direct numerical comparisons to the presented ambient measurements at the Sunset Crater field sites due to several differences, such as particle-size-selective sampling (PM_{10} versus total particle concentrations), sampling duration (24-hour averages versus a few hours), and site characteristics (urban versus rural settings). Qualitative and semiquantitative information gained from these measurements, however, can be useful. Specifically, the noted influence on measurement duration for the PM_{10} data could have a similar qualitative implications for RespiCon measurements (i.e., increases in the sampling duration for the RespiCon measurements during ambient conditions may yield lower average particle concentrations). Because nocturnal wind speeds can be notably lower than daytime values in desert terrains, the ambient resuspension potential might have been higher for the shorter duration, daytime RespiCon measurements of airborne particle concentration during ambient conditions relative to a 24-hour-averaged concentration. Depending on the day of the month, the 24-hour-averaged PM_{10} concentration at the same monitoring site varied by roughly factor of 4 to more than 10. This large amount of variability for

the relatively long 24-hour sampling duration may be explained at the lower end by the continuation of PM_{10} measurements during precipitation events and at the higher end by periods of increased dust generation from surrounding human activities. In contrast, ambient RespiCon measurements at Sunset Crater were not collected during or immediately after precipitation events and were set up in remote locations, absent of nearby human-induced dust generation. Coupled with the fact that the ambient Sunset Crater measurements represent a sparser data set, these points may explain why total airborne particle concentrations of more than 0.1 mg m^{-3} were measured at the Sunset Crater sites during ambient conditions. Given other factors contribute to significant variation in resuspension and measured airborne particle concentrations and preclude high levels of precision for comparisons, the RespiCon measurement results are in reasonable agreement with the results of other work.

CONCLUSION

Field measurements of airborne particle mass concentration were performed using a personal sampler under various levels of surface-disturbing conditions over different depositional environments at both volcanic and nonvolcanic sites near the Sunset Crater Volcano in northern Arizona. Under ambient conditions without human disturbance, the total airborne particle concentration ranged from 0.1 to 0.4 mg m^{-3} with most of the airborne mass attributed to particles with aerodynamic diameters less than 10 μm [0.00039 in]. Under light surface-disturbance activities, the total airborne particle concentration generally ranged from about 0.5 (or about 0.2 if the lowest result is included) to 2 mg m^{-3}, where concentrations up to 5 mg m^{-3} were only observed over fluvial deposits. For light disturbance conditions, about half of the airborne mass was associated with particles with aerodynamic diameters of 10–100 μm [0.00039–0.0039 in], although the higher recorded concentrations tended to correlate with a greater percentage of airborne mass from aerodynamic particle diameters greater than 10 μm

[0.00039 in]. During continuous heavy surface-disturbance activities, the total airborne particle concentration ranged from about 2 to 100 mg m^{-3} at volcanic sites and from about 2 to 10 mg m^{-3} at nonvolcanic sites. At the volcanic sites, a majority of the airborne mass resuspended from heavy disturbance was associated with particles with aerodynamic diameters of 10–100 μm [0.00039–0.0039 in]. At the nonvolcanic sites, about half of the airborne mass was attributed to particles with aerodynamic diameters of 10–100 μm [0.00039–0.0039 in]. As the surface-disturbing activity level increased, measurement uncertainties due to mass accumulation on the filters decreased, while variability in resuspension activities and ultimately in the measurement results increased. Thus, the measured airborne particle concentrations appeared more sensitive to the actions of the individual field investigator and specifics of the surface disturbing activity as the disturbance level increased. Higher wind speeds tended to increase airborne particle concentrations under ambient conditions. In contrast, higher wind speeds reduced the residence time of resuspended particles in the breathing zone for surface-disturbing activities and generally resulted in lower airborne particle concentrations measured by the individual performing the activity.

The surface-disturbing activity level was found to be the most influential factor affecting the measured airborne particle concentrations over basaltic tephra and other coarse-grained clastic deposits, which is consistent with the similar conclusion reached from other samples for silicic tephra deposits. Based on the measurements performed, the differences in airborne particle concentration over 900-year weathered volcanic basalt and nonvolcanic deposits appeared to be potentially significant only under heavy surface disturbances. Overall, the depositional environment (primarily non-reworked, reworked fluvial, reworked eolian) and percentage of near-surface mass that is resuspendible and inhalable were not as influential as other factors. A slight increase in the average airborne concentrations during ambient conditions was found above older nonvolcanic deposits, which tended to be finer-grained than

the Sunset Crater tephra deposits. An additional site with an extremely fine-grained deposit in a fluvial drainage system, however, exhibited increased susceptibility to airborne resuspension. Its ground surface material was not prevalent in the region, but its limited investigation determined that the effect of a substantial shift in the grain size distribution resulted in both noticeable and measurable increases in the airborne particle concentration in a field setting during surface-disturbing activities.

Acknowledgments

This paper describes work performed by the Center for Nuclear Waste Regulatory Analyses (CNWRA) for the U.S. Nuclear Regulatory Commission (NRC) under Contract No. NRC–02–02–012. The activities reported here were performed on behalf of the NRC Office of Nuclear Material Safety and Safeguards, Division of High-Level Waste Repository Safety. This paper is an independent product of the CNWRA and does not necessarily reflect the view or regulatory position of the NRC. The NRC staff views expressed herein are preliminary and do not constitute a final judgment or determination of the matters addressed or of the acceptability of a license application for a geologic repository at Yucca Mountain.

The authors are grateful to Sandra Watson, Mark Silver, and Paul Bertetti for providing timely support with the laboratory work and to John Roseberry for his assistance in the field. Brittain Hill, Danielle Wyrick, James Mancillas, Sitakanta Mohanty, Lauren Mulverhill, and John Trapp are thanked for reviewing and improving this paper. The support provided by Beverly Street on word processing during the preparation of this paper is also appreciated.

REFERENCES

American Conference of Governmental Industrial Hygienists. Threshold limit values for chemical substances and physical agents and biological exposure indices. Cincinnati, OH: American Conference of Governmental Industrial Hygienists; 1995.

Amos RC. Sunset Crater, Arizona: Evidence for a large magnitude strombolian eruption. Tempe, AZ: Arizona State University; 1986. Master's thesis.

Anspaugh LR, Shinn JH, Phelps PL, Kennedy, NC. Resuspension and redistribution of Plutonium in soils. Health Phys 29:571–582; 1975.

Anspaugh LR, Simon SL, Gordeev KI, Likhtarev IA, Maxwell RM, Shinkarev SM. Movement of radionuclides in terrestrial ecosystems by physical process. Health Phys 82(5):669–679; 2002.

Benke RR, Hill BE, Hooper DM. Fluvial redistribution of contaminated tephra: Description of an abstracted model. In: Global progress toward safe disposal. Proceedings of the 11th International High-Level Radioactive Waste Management Conference. La Grange Park, IL: American Nuclear Society; 2006: 958–962.

Blong, B. Volcanic hazards risk assessment. In: Scarpa R, Tilling RI, eds. Monitoring and mitigation of volcanic hazards. Berlin: Springer; 1996: 675–698.

Buist AS, Johnson LR, Vollmer WM, Sexton GJ, Kanarek PH. Acute effects of volcanic ash from Mount Saint Helens on lung function in children. Am Rev Respir Dis 127(6): 714–9; 1983.

Feather GA, Chen BT. Design and use of a settling chamber for sampler evaluation under calm-air conditions. Aerosol Sci Technol 37:261–270; 2003.

Hamilton IS, Arno MG, Rock JC, Berry RO, Poston JW, Sr., Cezeaux JR, Park JM. Radiological assessment of petroleum pipe scale from pipe-rattling operations. Health Phys 87(4):392–396; 2004.

Hill BE, Connor CB, Weldy J, Franklin N. Methods for quantifying hazards from basaltic tephra-fall eruptions. Proceedings of the Cities on Volcanoes 2 Conference, Auckland, New Zealand, February 12–14, 2001. Stewart C, ed. Lower Hutt, New Zealand: Institute of Geological and Nuclear Sciences Limited. Institute of Geological and Nuclear Sciences Information Series 49; 2000: 158.

Holm RF, Moore RB. Holocene scoria cone and lava flows at Sunset Crater, northern Arizona. Geological Society of America Centennial Field Guide–Rocky Mountain Section. DNAG Project; 2:393–397; 1987.

Horwell CJ, Baxter PJ. The respiratory health hazards of volcanic ash: A review for volcanic risk mitigation. Bull Volcanol 69:1–24; 2006.

Horwell CJ, Sparks RSJ, Brewer TS, Llewellin EW, Williamson, BJ. Characterization of respirable volcanic ash from the Soufrière Hills volcano, Montserrat, with implications for human health hazards. Bull Volcanol 65:346–362; 2003.

International Commission on Radiological Protection. Human respiratory tract model for radiological protection. Tarrytown, NY: Elsevier Science, Inc; ICRP Publication 66; Ann ICRP 24 (1–3); 1994.

Li SN, Lundgren DA, Rovell-Rixx D. Evaluation of six inhalable aerosol samplers. Amer Ind Hyg Assoc J 61: 506–516; 2000.

Mohanty S, Benke R, Codell R, Compton K, Esh D, Gute D, Howard L, McCartin T, Pensado O, Smith M, Adams G, Ahn T, Bertetti P, Browning L, Cragnolino G, Dunn D, Fedors R, Hill B, Hooper D, LaPlante P, Leslie B, Nes R, Ofoegbu G, Pabalan R, Rice R, Rubenstone J, Trapp J, Winfrey B, Yang L. Risk analysis for risk insights progress report. San Antonio, TX: Center for Nuclear Waste Regulatory Analyses; 2005. Available at: http://www.nrc.gov/reading-rm/adams.html.

Mohanty S, McCartin TJ, Esh DW. Total-system performance assessment (TPA) version 4.0 code: Module descriptions and user's guide. San Antonio, TX: Center for Nuclear Waste Regulatory Analyses; 2002. Available at: http://www.nrc.gov/reading-rm/adams.html.

Moore KR, Duffell H, Nicholl A, Searl A. Monitoring of airborne particulate matter during the eruption of the Soufrière Hills Volcano, Montserrat. The eruption of the Soufrière Hills Volcano, Montserrat, from 1995 to 1999. Druitt TH, Kokelaar BP,eds. London: The Geological Society of London. Geological Society, London, Memoirs; 2002: 21:557–566.

Rando R, Poovey H, Mokadam D, Brisolara J. Field performance of the RespiCon for size-selective sampling of industrial wood processing dust. J Occup Environ Hyg 2(4):219–226; 2005.

Searl A, Nicholl A, and Baxter PJ. Assessment of the exposure of islanders to ash from the Soufriere Hills Volcano, Montserrat, British West Indies. J Occup Environ Med 59:523–531; 2002.

Sellers WD, Hill RH, eds. Arizona climate. Tucson, AZ: The University of Arizona Press; 1974.

Smiley TL. The geology and dating of Sunset Crater, Flagstaff, Arizona. Ninth field conference, New Mexico Geological Society, Field conference guidebook. Socorro, NM; 1958: 186–190.

Tanaka KL, Onstott TC, Shoemaker EM. Magnetostratigraphy of the San Francisco Volcanic Field, Arizona. US Geol S Bul 1929; 1990.

Tatum V, Ray AE, Rovell-Rixx D. Performance of the RespiCon personal aerosol sampler in forest products industry workplaces. Amer Ind Hyg Assoc 63:311–316; 2002.

Till JE, Meyer HR, eds. NUREG/CR–3332, Radiological assessment. A textbook on environmental dose analysis. Washington, DC: NRC; 1983. Available at: http://www.nrc.gov/reading-rm/adams.html.

TSI Incorporated. Health-based particle-size-selective sampling. TSI Application Note ITI–050. St. Paul, MN: TSI Incorporated; 2006. Available at: http://www.tsi.com.

TSI Incorporated. Revised correction factor for the RESPICON™ particle sampler. TSI Application Note ITI-078. St. Paul, MN: TSI Incorporated; 2001. Available at: http://www.tsi.com.

Wiggs GFS. Sediment mobilisation by the wind. In: Thomas DSG, ed. Arid zone geomorphology: Process, form and change in drylands, 2nd ed. New York, NY: Wiley & Sons; 1997: 351–372.

FOOTNOTES

*Center for Nuclear Waste Regulatory Analyses, Southwest Research Institute®, 6220 Culebra Road, San Antonio, TX 78238-5166

†U.S. Nuclear Regulatory Commission, Division of High-Level Waste Repository Safety, Two White Flint North, 11545 Rockville Pike, Washington, DC, 20555

‡Department of Earth, Material, and Planetary Sciences, Southwest Research Institute®, 6220 Culebra Road, San Antonio, TX 78238-5166

FIGURE CAPTIONS

Fig. 1 Airborne particle sampling sites. In general, the region consists of bare tephra or lava (black), forests (green), semi-arid to arid terrain with grasses and thin soil cover (light blue), oxidized basalt with high iron content (red to pink), and bare limestone and sandstone with eolian sand or disturbed and exposed land (yellow to white).

Fig. 2 Location of surface samples centered around ambient airborne particle measurement location. Inner ring is 2 m [6.6 ft] from center. Outer ring is 4 m [13 ft] from center.

Fig. 3 (a) Total airborne particle concentrations, as shown in Table 2, and (b) airborne particle size distributions for ambient conditions. Identical labels for surface materal type imply separate measurements on different days at the same site, except for the nonvolcanic, primarily nonreworked type (refer to Materials and Methods section). Total flow checks were performed for all measurements. Particle size information is not presented for the three measurements without premeasurement verification of stage flows. Error bars represent uncertainty estimates for 1 standard deviation.

Fig. 4 (a) Total airborne particle concentrations, as shown in Table 3, and (b) airborne particle size distributions for light disturbance conditions. Identical labels for surface materal type imply separate measurements on different days at the same site, except for the nonvolcanic, primarily nonreworked type (refer to Materials and Methods section). Refer to the Discussion section for an explanation on why particle size information is not presented for one measurement. Error bars represent uncertainty estimates for 1 standard deviation.

Fig. 5 (a) Total airborne particle concentrations, as shown in Table 4, and (b) airborne particle size distributions for heavy disturbance conditions. Identical labels for surface materal type imply separate measurements on different days at the same site, except for the nonvolcanic, primarily nonreworked type (refer to Materials and Methods section). Error bars represent uncertainty estimates for 1 standard deviation.

Fig. 6 Images of surface samples for volcanic sites: (a) V-P, (b) V-F channel, (c) V-F banks, and (d) V-E. Surface samples were collected to a depth of approximately 1 cm [0.4 in].

Fig. 7 Images of surface samples for nonvolcanic sites: (a) N-Pa, (b) N-Ps, (c) N-F, and (d) N-E. Except for Site N-Ps, the surface samples were collected to a depth of approximately 1 cm [0.4 in]. At Site N-Ps, the depth of loose surface material was much less than 1 cm [0.4 in], and the surface sample consisted of the loose material present within an area of 4 m^2 [11 ft^2].

Fig. 8 Surface-sample image for the very fine-grained deposit at Site Extra-F. The surface sample was collected to a depth of approximately 1 cm [0.4 in].

Fig. 9 Grain-size distributions for surface samples at the volcanic sites (refer to Fig. 6 for images). Sample mass collected in the pan is plotted with a grain size of 4.75 phi. Grain diameter in millimeters equals $2^{-(\text{grain size in phi})}$.

Fig. 10 Grain-size distributions for surface samples at the nonvolcanic sites (refer to Figs. 7 and 8 for images). Sample mass collected in the pan is plotted with a grain size of 4.75 phi. Grain diameter in millimeters equals $2^{-(\text{grain size in phi})}$.

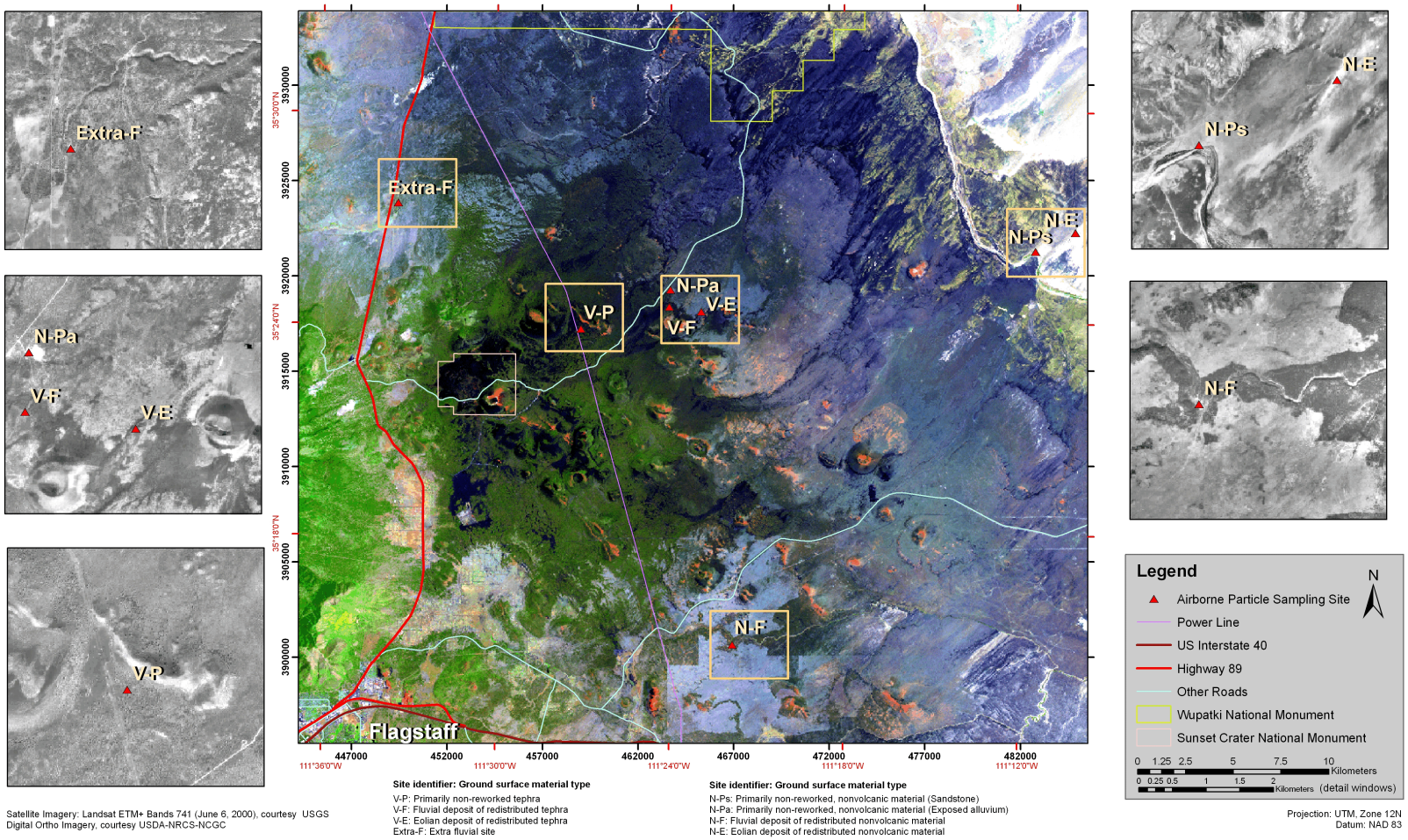

Satellite Imagery: Landsat ETM+ Bands 741 (June 6, 2000), courtesy USGS
Digital Ortho Imagery, courtesy USDA-NRCS-NCGC

Site identifier: Ground surface material type

V-P: Primarily non-reworked tephra
V-F: Fluvial deposit of redistributed tephra
V-E: Eolian deposit of redistributed tephra
Extra-F: Extra fluvial site

Site identifier: Ground surface material type

N-Ps: Primarily non-reworked, nonvolcanic material (Sandstone)
N-Pa: Primarily non-reworked, nonvolcanic material (Exposed alluvium)
N-F: Fluvial deposit of redistributed nonvolcanic material
N-E: Eolian deposit of redistributed nonvolcanic material

Projection: UTM, Zone 12N
Datum: NAD 83

Fig. 1

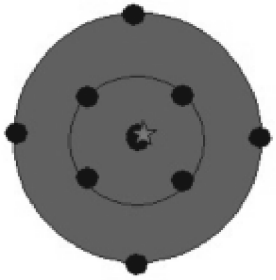

★ Location of Ambient Airborne Particle Measurement

● Surface Sample Location

Fig. 2

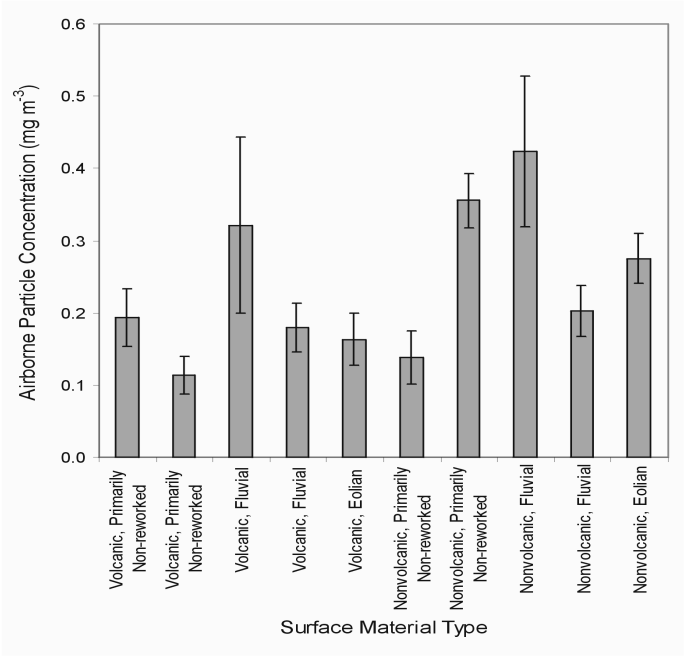
Airborne Particle Concentration (mg m-3)
0.0
0.1
0.2
0.3
0.4
0.5
0.6
Volcanic, Primarily Non-reworked
Volcanic, Primarily Non-reworked
Volcanic, Fluvial
Volcanic, Fluvial
Volcanic, Eolian
Nonvolcanic, Primarily Non-reworked
Nonvolcanic, Primarily Non-reworked
Nonvolcanic, Fluvial
Nonvolcanic, Fluvial
Nonvolcanic, Eolian
Surface Material Type

(a)

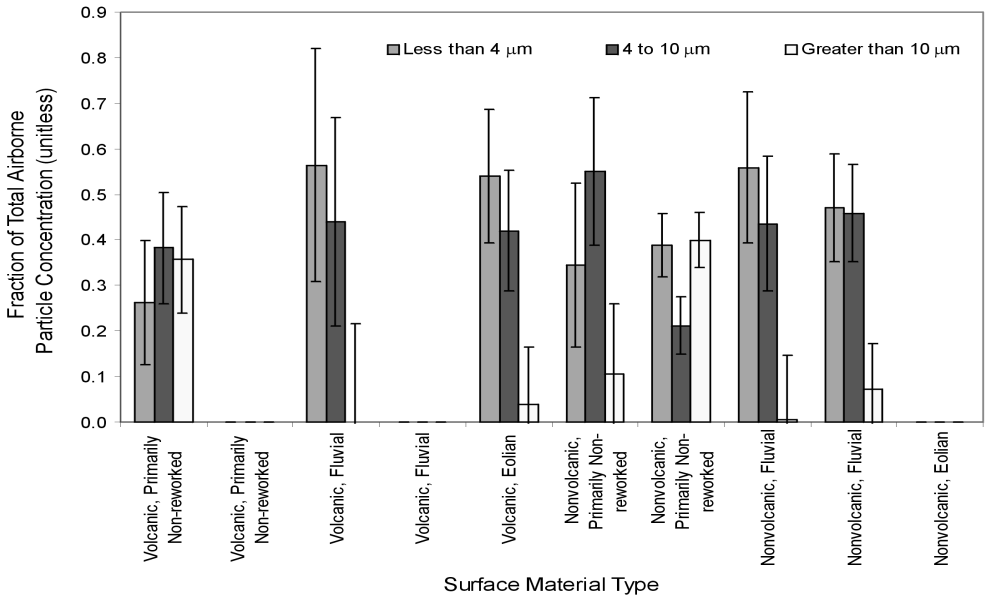
Fraction of Total Airborne Particle Concentration (unitless)
0.0
0.1
0.2
0.3
0.4
0.5
0.6
0.7
0.8
0.9
Less than 4 μm
4 to 10 μm
Greater than 10 μm
Volcanic, Primarily Non-reworked
Volcanic, Primarily Non-reworked
Volcanic, Fluvial
Volcanic, Fluvial
Volcanic, Eolian
Nonvolcanic, Primarily Non-reworked
Nonvolcanic, Primarily Non-reworked
Nonvolcanic, Fluvial
Nonvolcanic, Fluvial
Nonvolcanic, Eolian
Surface Material Type

(b)

Fig. 3

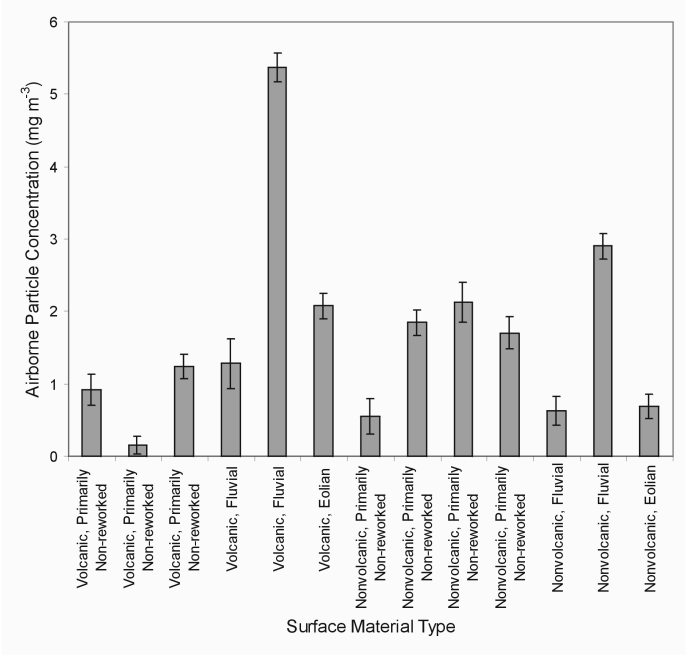
Airborne Particle Concentration (mg m-3)
0
1
2
3
4
5
6
Volcanic, Primarily Non-reworked
Volcanic, Primarily Non-reworked
Volcanic, Primarily Non-reworked
Volcanic, Fluvial
Volcanic, Fluvial
Volcanic, Eolian
Nonvolcanic, Primarily Non-reworked
Nonvolcanic, Primarily Non-reworked
Nonvolcanic, Primarily Non-reworked
Nonvolcanic, Primarily Non-reworked
Nonvolcanic, Fluvial
Nonvolcanic, Fluvial
Nonvolcanic, Eolian
Surface Material Type

(a)

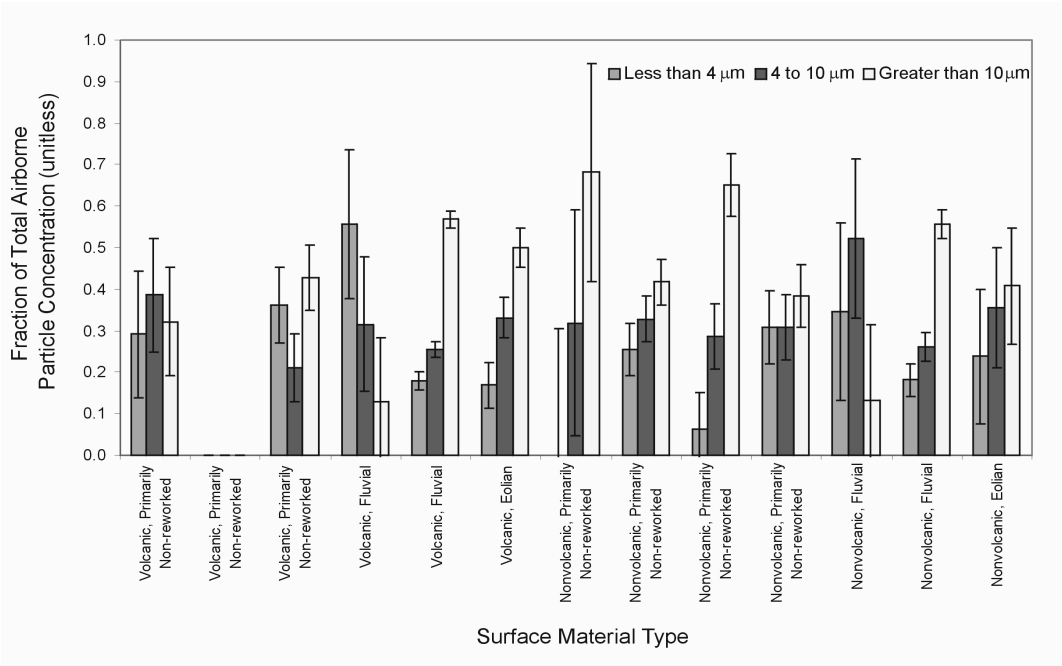
Fraction of Total Airborne Particle Concentration (unitless)
0.0
0.1
0.2
0.3
0.4
0.5
0.6
0.7
0.8
0.9
1.0
Less than 4 μm
4 to 10 μm
Greater than 10μm
Volcanic, Primarily Non-reworked
Volcanic, Primarily Non-reworked
Volcanic, Primarily Non-reworked
Volcanic, Fluvial
Volcanic, Fluvial
Volcanic, Eolian
Nonvolcanic, Primarily Non-reworked
Nonvolcanic, Primarily Non-reworked
Nonvolcanic, Primarily Non-reworked
Nonvolcanic, Primarily Non-reworked
Nonvolcanic, Fluvial
Nonvolcanic, Fluvial
Nonvolcanic, Eolian
Surface Material Type

(b)

Fig. 4

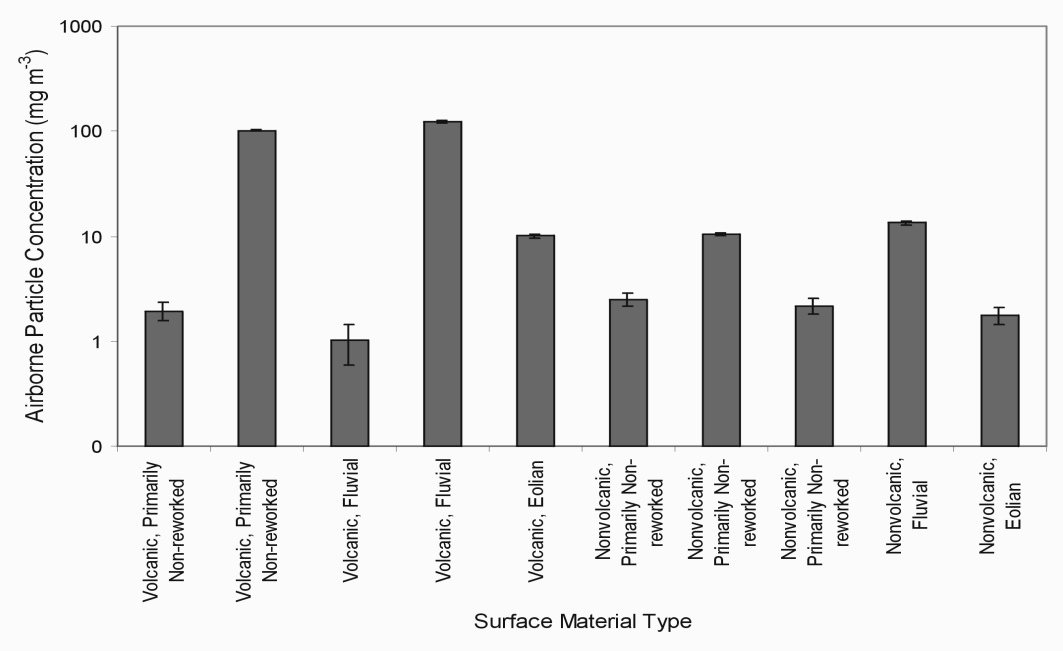
Airborne Particle Concentration (mg m-3)
1000
100
10
1
0
Volcanic, Primarily Non-reworked
Volcanic, Primarily Non-reworked
Volcanic, Fluvial
Volcanic, Fluvial
Volcanic, Eolian
Nonvolcanic, Primarily Non-reworked
Nonvolcanic, Primarily Non-reworked
Nonvolcanic, Primarily Non-reworked
Nonvolcanic, Fluvial
Nonvolcanic, Eolian
Surface Material Type

(a)

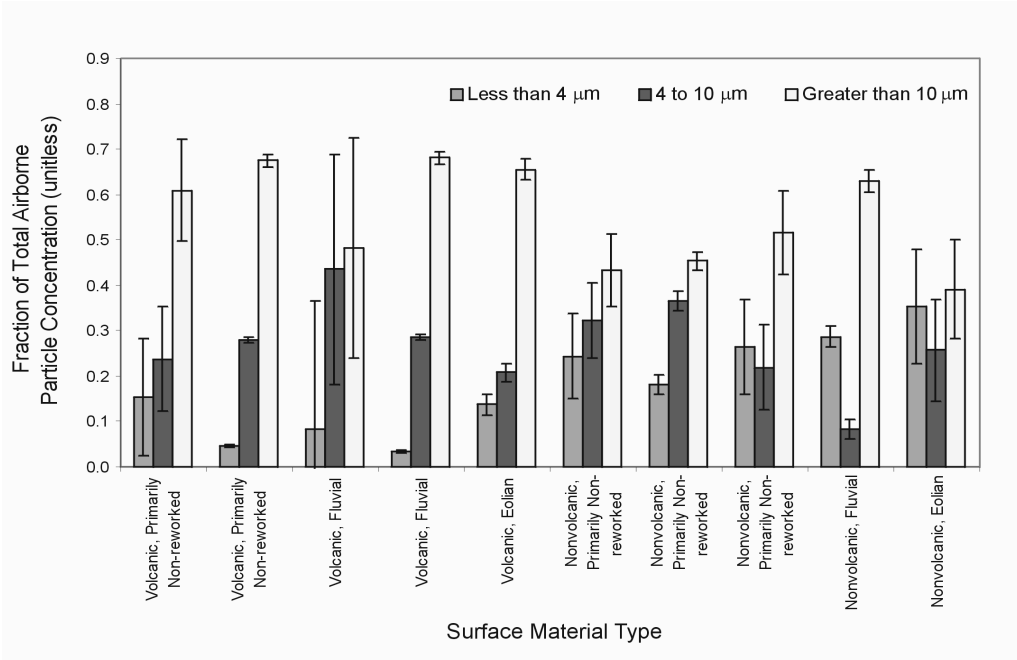
Fraction of Total Airborne Particle Concentration (unitless)
0.9
0.8
0.7
0.6
0.5
0.4
0.3
0.2
0.1
0.0
Less than 4 μm
4 to 10 μm
Greater than 10 μm
Volcanic, Primarily Non-reworked
Volcanic, Primarily Non-reworked
Volcanic, Fluvial
Volcanic, Fluvial
Volcanic, Eolian
Nonvolcanic, Primarily Non-reworked
Nonvolcanic, Primarily Non-reworked
Nonvolcanic, Primarily Non-reworked
Nonvolcanic, Fluvial
Nonvolcanic, Eolian
Surface Material Type

(b)

Fig. 5

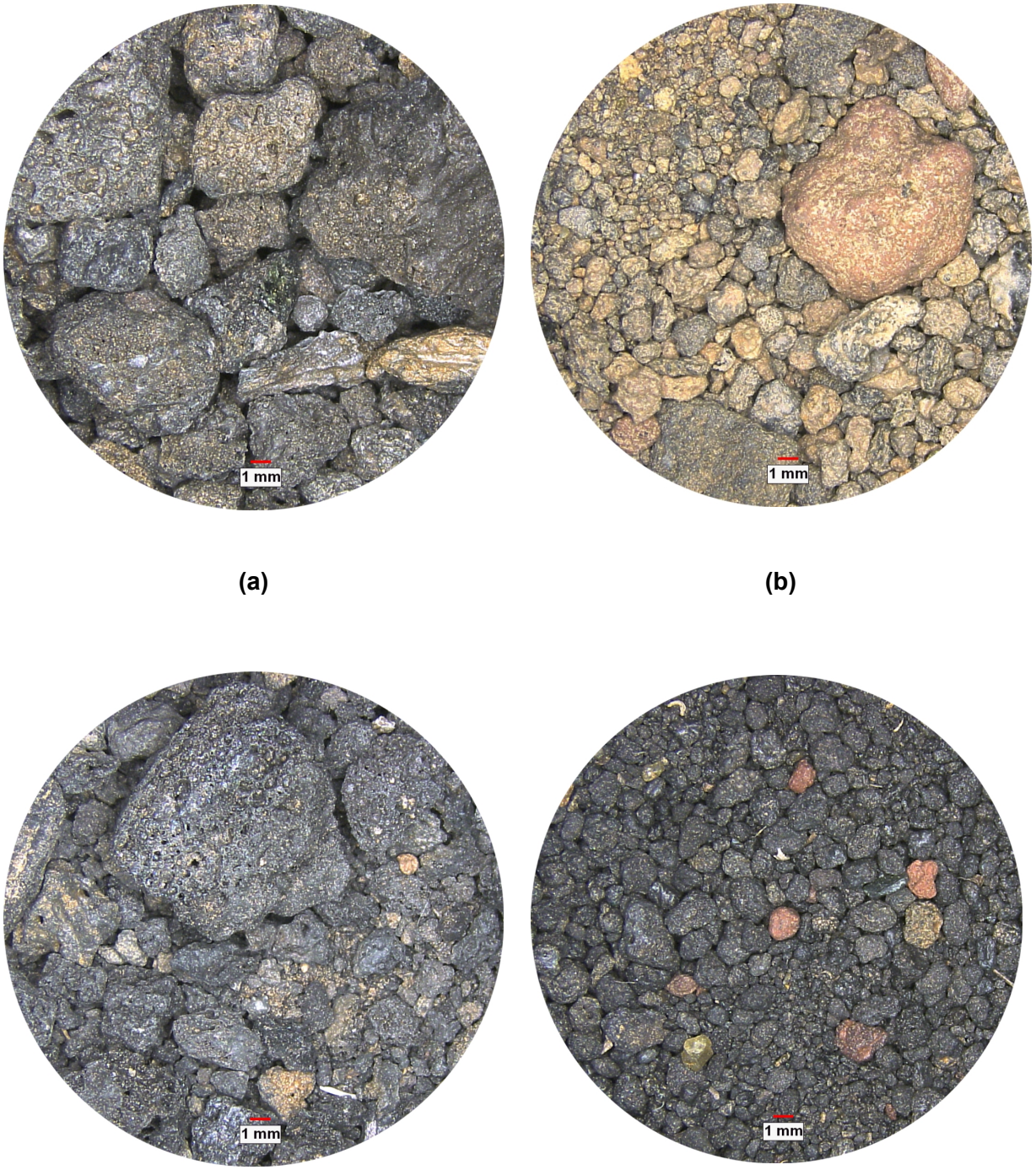

(a) (b)

(c) (d)

Fig. 6

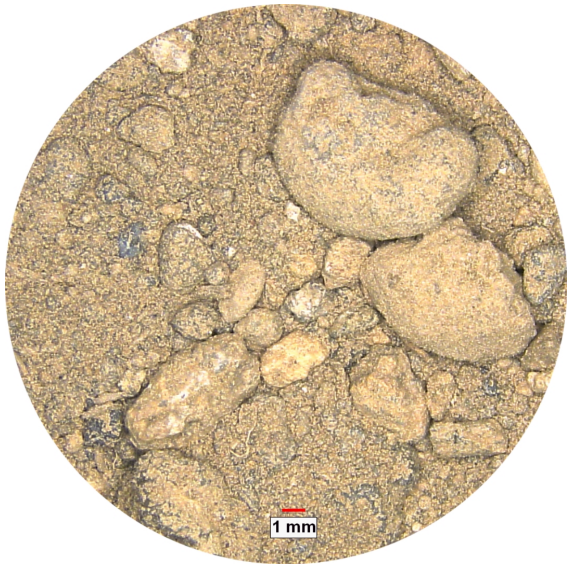

(a)

(b)

(c)

(d)

Fig. 7

Fig. 8

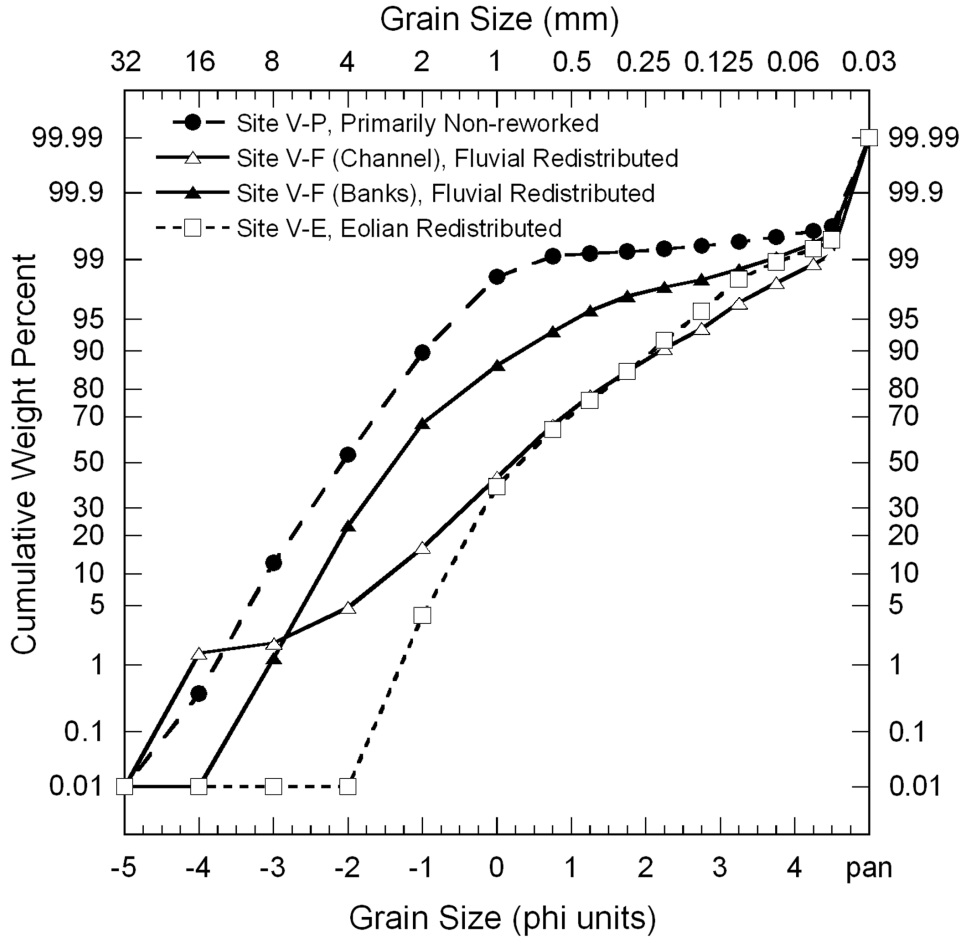
Grain Size (mm)
32
16
8
4
2
1
0.5
0.25
0.125
0.06
0.03
Site V-P, Primarily Non-reworked
Site V-F (Channel), Fluvial Redistributed
Site V-F (Banks), Fluvial Redistributed
Site V-E, Eolian Redistributed
Cumulative Weight Percent
99.99
99.9
99
95
90
80
70
50
30
20
10
5
1
0.1
0.01
-5
-4
-3
-2
-1
0
1
2
3
4
pan
Grain Size (phi units)

Fig. 9

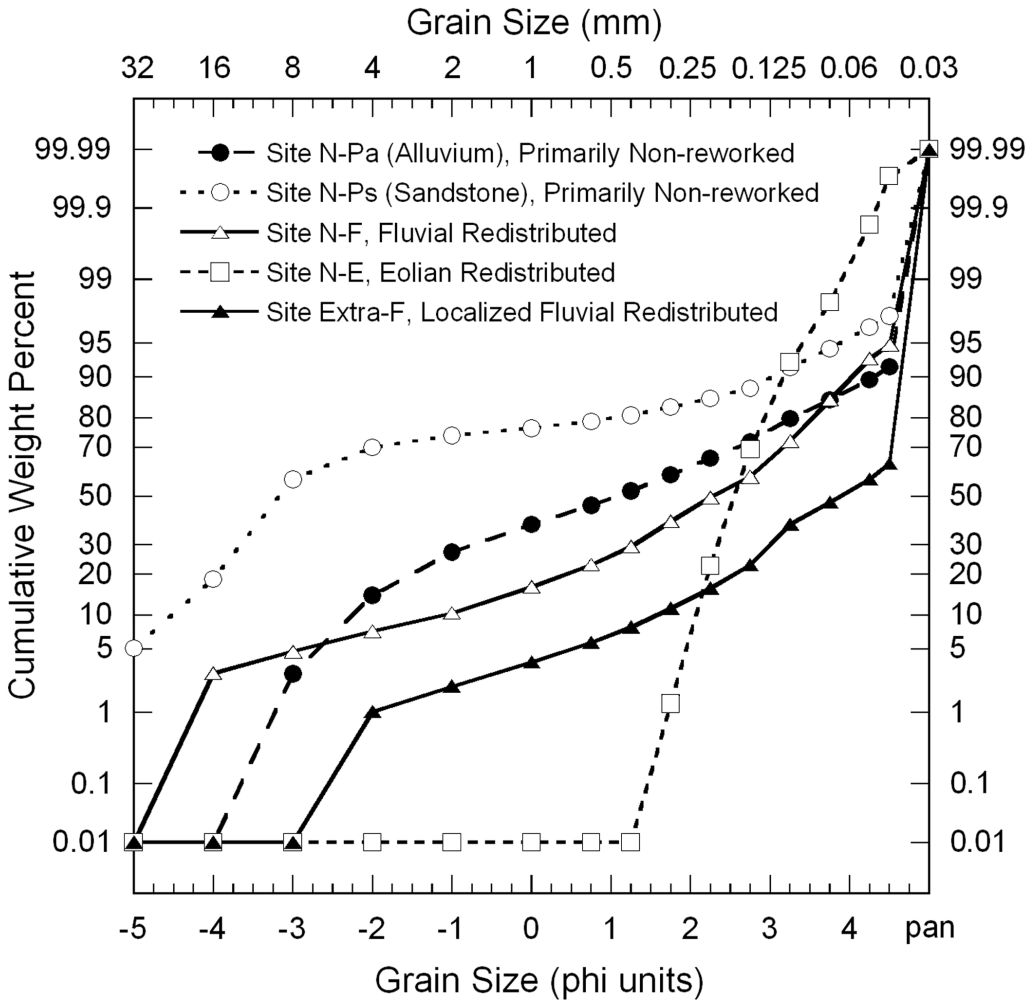
Grain Size (mm)
32
16
8
4
2
1
0.5
0.25
0.125
0.06
0.03
Site N-Pa (Alluvium), Primarily Non-reworked
Site N-Ps (Sandstone), Primarily Non-reworked
Site N-F, Fluvial Redistributed
Site N-E, Eolian Redistributed
Site Extra-F, Localized Fluvial Redistributed
Cumulative Weight Percent
99.99
99.9
99
95
90
80
70
50
30
20
10
5
1
0.1
0.01
-5
-4
-3
-2
-1
0
1
2
3
4
pan
Grain Size (phi units)

Fig. 10

Table 1. Measurement classes for airborne particle concentrations.

Surface Disturbance Level	Ground Surface Material Type & Depositional Environment					
	Volcanic			Nonvolcanic		
	Primarily Non-reworked	Fluvial Redistributed	Eolian Redistributed	Primarily Non-reworked	Fluvial Redistributed	Eolian Redistributed
Ambient	1	4	7	10	13	16
Light	2	5	8	11	14	17
Heavy	3	6	9	12	15	18

Table 2. Total airborne particle measurement results for ambient conditions (Fig. 3). In some cases, separate measurements were performed at the same site on different days.

Site	Site Description	Airborne Particle Concentration (mg m^{-3})	± 1σ Uncertainty (mg m^{-3})	Average Wind Speed[a] (mi h^{-1})
V-P	Volcanic, Primarily Non-reworked	0.19	0.04	6.5
V-P	Volcanic, Primarily Non-reworked	0.11	0.03	5.3
V-F	Volcanic, Fluvial	0.32	0.12	11.6
V-F	Volcanic, Fluvial	0.18	0.03	4.6
V-E	Volcanic, Eolian	0.16	0.04	4.7
N-Pa	Nonvolcanic, Primarily Non-reworked	0.14	0.04	3.7
N-Ps	Nonvolcanic, Primarily Non-reworked	0.36	0.04	5.8
N-F	Nonvolcanic, Fluvial	0.42	0.10	4.6
N-F	Nonvolcanic, Fluvial	0.20	0.04	4.6
N-E	Nonvolcanic, Eolian	0.28	0.03	6.0

[a]Daily average values reported for Flagstaff, AZ (Flagstaff Pulliam Airport) by the U.S. Department of Commerce, National Oceanic and Atmospheric Administration, National Climatic Data Center (1 mi h^{-1} = 0.447 m s^{-1})

Table 3. Total airborne particle concentration measurement results for light disturbance conditions (Fig. 4). In some cases, separate measurements were performed at the same site on different days.

Site	Site Description	Airborne Particle Concentration (mg m^{-3})	± 1σ Uncertainty (mg m^{-3})	Average Wind Speed[a] (mi h^{-1})
V-P	Volcanic, Primarily Non-reworked	0.92	0.21	7.4
V-P	Volcanic, Primarily Non-reworked	0.15	0.12	9.9
V-P	Volcanic, Primarily Non-reworked	1.2	0.2	5.3
V-F	Volcanic, Fluvial	1.3	0.3	11.6
V-F	Volcanic, Fluvial	5.4	0.2	4.6
V-E	Volcanic, Eolian	2.1	0.2	4.7
N-Pa	Nonvolcanic, Primarily Non-reworked	0.5	0.2	10.4
N-Pa	Nonvolcanic, Primary Non-reworked	1.8	0.2	3.7
N-Ps	Nonvolcanic, Primarily Non-reworked	2.1	0.3	6.0
N-Ps	Nonvolclanic, Primarily Non-reworked	1.7	0.2	5.8
N-F	Nonvolcanic, Fluvial	0.6	0.2	4.6
N-F	Nonvolcanic, Fluvial	2.9	0.2	4.6
N-E	Nonvolcanic, Eolian	0.7	0.2	6.0

[a]Daily average values reported for Flagstaff, AZ (Flagstaff Pulliam Airport) by the U.S. Department of Commerce, National Oceanic and Atmospheric Administration, National Climatic Data Center (1 mi h^{-1} = 0.447 m s^{-1})

Table 4. Total airborne particle concentration measurement results for heavy disturbance conditions (Fig. 5). In some cases, separate measurements were performed at the same site on different days.

Site	Site Description	Airborne Particle Concentration (mg m^{-3})	+/- 1σ Uncertainty (mg m^{-3})	Average Wind Speed[a] (mi h^{-1})
V-P	Volcanic, Primarily Non-reworked	1.9	0.4	7.4
V-P	Volcanic, Primarily Non-reworked	101.7	2.1	5.3
V-F	Volcanic, Fluvial	1.0	0.4	16.9
V-F	Volcanic, Fluvial	123.4	2.5	4.6
V-E	Volcanic, Eolian	10.1	0.4	4.7
N-Pa	Nonvolcanic, Primarily Non-reworked	2.5	0.3	3.7
N-Ps	Nonvolcanic, Primarily Non-reworked	10.4	0.4	6.0
N-F	Nonvolcanic, Fluvial	2.2	0.3	4.6
N-F	Nonvolcanic, Fluvial	13.4	0.5	4.6
N-E	Nonvolcanic, Eolian	1.8	0.3	6.0

[a]Daily average values reported for Flagstaff, AZ (Flagstaff Pulliam Airport) by the U.S. Department of Commerce, National Oceanic and Atmospheric Administration, National Climatic Data Center (1 mi h^{-1} = 0.447 m s^{-1})

Table 5. Site description and percent of grain mass in surface sample with diameters less than 106 µm [0.00417 in]. Figs. 9 and 10 display the grain-size distributions.

Site Identifier	Ground Surface Material Type	Description	Percent of Grain Mass Less Than 106 µm [0.00417 in]
V-P[a]	Volcanic, Primarily Non-reworked	Primarily non-reworked implies an *in situ* deposit or tephra that has not been transported by erosional processes from the place of original deposition. Non-reworked or pristine tephra is glassy and vesicular representing volcanic fragments that have fallen to the ground in a solid condition.	0.6
V-F[a]	Volcanic, Fluvial Channel[b]	Samples collected from the channel and banks of a small wash (ephemeral stream). Friction and impact during transport by running water may abrade and mechanically break tephra particles. Tephra may be mixed with other materials. The channel deposit was not well sorted.	3
	Volcanic, Fluvial Banks[b]		1
V-E[a]	Volcanic, Eolian	Coppice dune environment where wind or eolian processes produce fine-size, well-sorted, and well-rounded tephra grains. Clay content (illite, mica, and kaolinite) of about 4 percent by weight is greater than the negligible clay content in pristine, non-reworked tephra.	2

Table 5. (continued) Site description and percent of grain mass in surface sample with diameters less than 106 µm [0.00417 in]. Figs. 9 and 10 display the grain-size distributions.

Site Identifier	Ground Surface Material Type	Description	Percent of Grain Mass Less Than 106 µm [0.00417 in]
N-Pa	Nonvolcanic, Primarily Non-reworked (alluvium)[c]	Unconsolidated and unsorted sediment of exposed alluvial pebbles, sand, and silt derived from basaltic volcanism that predates the Sunset Crater eruption. Alluvium in the Sunset Crater area can be composed of nonvolcanic material from the Moenkopi and Kaibab Formations, volcanic material of a nonbasaltic composition including San Francisco Mountain and andesitic to rhyolitic lava domes, and basalt. The amount of ferromagnesian components (plagioclase, augite, and olivine) of about 70 percent by weight in the alluvium is similar to the total amount in pristine Sunset Crater tephra. The alluvium, however, had a higher quartz and calcite content (together about 10 percent by weight), compared to negligible amounts in pristine Sunset Crater tephra. Lower amounts of amorphous glass (about 15 percent by weight) were also found in the alluvium.	20
N-Ps	Nonvolcanic, Primarily Non-reworked (sandstone)	Calcareous sandstone of the Moenkopi Formation primarily composed of quartz and calcite (over 80 percent by weight) with lesser amounts of clay (predominantly kaolinite with smaller amounts of illite and mica), potassium feldspar, dolomite, and hematite.	8

Table 5. (continued) Site description and percent of grain mass in surface sample with diameters less than 106 µm [0.00417 in]. Figs. 9 and 10 display the grain-size distributions.

Site Identifier	Ground Surface Material Type	Description	Percent of Grain Mass Less Than 106 µm [0.00417 in]
N-F	Nonvolcanic, Fluvial	Fluvially redistributed deposit of pebbles, sand, and silt from San Francisco Wash, an ephemeral stream that drains a larger area including limestone and dolostone from the Kaibab Formation exposed to the southwest. In addition to fragments of the Kaibab Formation, the sample also consists of detrital quartz and feldspar, fragments of the Moenkopi Formation, and some basaltic lava fragments that predate the Sunset Crater eruption. Sunset Crater tephra is a minor component.	27
N-E	Nonvolcanic, Eolian	Sand and silt redistributed from eolian processes. Dune samples were mainly composed of quartz with lesser amounts of potassium feldspar and plagioclase. Tephra from either the Merriam Crater or Sunset Crater eruption is a minor component.	8
Extra-F	Extra nonvolcanic fluvial deposit	Fluvially redistributed material composed of fine-grained sand, silt, and clay dropped from suspension after stream flow events. Although time limitations restricted scouting of areas around this extra measurement site, the mainly silt-sized deposit seemed localized to where an unpaved forest route road crossed Deadman Wash, northwest of Sunset Crater. The fluvial deposit originates from the San Francisco Mountain drainage system, located west of Sunset Crater and U.S. Interstate 40. Compared to the basaltic tephra of Sunset Crater, the San Francisco Mountain area consists mainly of andesite of a much older igneous origin. Other material (e.g., glacial deposits) may also be present in the drainage system and available for fluvial transport.	62

Table 5. (continued) Site description and percent of grain mass in surface sample with diameters less than 106 μm [0.00417 in]. Figs. 9 and 10 display the grain-size distributions.

[a]Sunset Crater tephra is basaltic and dark-colored due to a ferromagnesian mineral composition. X-ray diffraction analysis in the laboratory has identified calcium-rich plagioclase, amorphous (glass), augite, and olivine components at approximately 39, 28, 17, and 13 percent by weight, respectively.

[b]Surface samples of channel and bank deposits at the fluvial volcanic site were collected and processed separately. The fluvial channel was approximately 3-m [10-ft] wide with banks about 2-m [7-ft] high.

[c]The term “primarily non-reworked” is used to indicate that the deposit is not in an active region of fluvial or eolian erosion and redistribution.

APPENDIX

Airborne Particle Concentration Calculations and Measurement Uncertainty Analysis

Measurement uncertainty of the microbalance was quantified by performing a repeatability study using a 10-mg traceable weight standard (10 mg Check Weight Class 1, Mettler-Toledo, Inc., Columbus, OH 43240). The standard deviation for measurement of filter mass was determined to be 0.024 mg. The relative measurement uncertainty of the flow rate meter was assigned the maximum allowable error of 2 percent, which was used as an acceptance criterion during its calibration. Uncertainties in sampling time were negligible and were not included in the error propagation calculations. Symbols, descriptions, and units for the calculational inputs are displayed in Table A–1. Table A–2 shows the symbols and descriptions for the calculational outputs. Each equation for airborne particle concentration is paired with the equation for its corresponding uncertainty in Table A–3.

Table A–1. Description of symbols for calculational inputs.

Symbol	Description	Units
$m_{1,i}$	Initial mass of Stage 1 (upper) filter	g
$m_{2,i}$	Initial mass of Stage 2 (middle) filter	g
$m_{3,i}$	Initial mass of Stage 3 (lower) filter	g
$m_{1,f}$	Final postsampling mass of Stage 1 (upper) filter	g
$m_{2,f}$	Final postsampling mass of Stage 2 (middle) filter	g
$m_{3,f}$	Final postsampling mass of Stage 3 (lower) filter	g
$f_{1,\text{nominal}}$	Nominal air flow rate through Stage 1 at standard temperature and pressure (defined to be 2.667 L min^{-1})	L min^{-1}
$f_{2,\text{nominal}}$	Nominal air flow rate through Stage 2 at standard temperature and pressure (defined to be 0.333 L min^{-1})	L min^{-1}
$f_{3,\text{nominal}}$	Nominal air flow rate through Stage 3 at standard temperature and pressure (defined to be 0.111 L min^{-1})	L min^{-1}
$f_{\text{total,nominal}}$	Nominal total air flow rate at standard temperature and pressure	L min^{-1}
$f_{\text{total,sampling}}$	Sampling total air flow rate at field temperature and pressure	L min^{-1}
t_{sampling}	Sampling time of airborne particle measurement	min
σ_m	Standard deviation for measurement of filter mass	g
$\frac{\sigma_f}{f}$	Standard deviation of measured air flow rate relative to the measured flow rate	unitless

Table A–2. Description of symbols for calculational outputs.

Symbol	Description (1 μm = 0.000039 in)	Units
$C_{<100}$	Airborne concentration of particles with aerodynamic diameters less than 100 μm	mg m^{-3}
$C_{<10}$	Airborne concentration of particles with aerodynamic diameters less than 10 μm	mg m^{-3}
$C_{<4}$	Airborne concentration of particles with aerodynamic diameters less than 4 μm	mg m^{-3}
$C_{4–10}$	Airborne concentration of particles with aerodynamic diameters between 4 and 10 μm	mg m^{-3}
$C_{10–100}$	Standard deviation of airborne concentration for particles with aerodynamic diameters between 10 and 100 μm	mg m^{-3}
$\sigma_{C,<100}$	Standard deviation of airborne concentration for particles with aerodynamic diameters less than 100 μm	mg m^{-3}
$\sigma_{C,<10}$	Standard deviation of airborne concentration for particles with aerodynamic diameters less than 10 μm	mg m^{-3}
$\sigma_{C,<4}$	Standard deviation of airborne concentration for particles with aerodynamic diameters less than 4 μm	mg m^{-3}
$\sigma_{C,4–10}$	Standard deviation of airborne concentration for particles with aerodynamic diameters between 4 and 10 μm	mg m^{-3}
$\sigma_{C,10–100}$	Standard deviation of airborne concentration for particles with aerodynamic diameters between 10 and 100 μm	mg m^{-3}

Table A–3. Equations for airborne particle concentration and its uncertainty.

$$C_{<100} = \frac{\left(m_{1,f} - m_{1,i}\right) + \left(m_{2,f} - m_{2,i}\right) + \left(m_{3,f} - m_{3,i}\right)}{f_{\text{total,sampling}} \times \dfrac{f_{1,\text{nominal}} + f_{2,\text{nominal}} + f_{3,\text{nominal}}}{f_{\text{total,nominal}}} \times t_{\text{sampling}}} \times \frac{1000\ \text{mg}}{\text{g}} \times \frac{1000\ \text{L}}{\text{m}^3}$$

$$\sigma_{C,<100} = C_{<100} \times \sqrt{6\left(\frac{\sigma_m}{m_{1,f} - m_{1,i} + m_{2,f} - m_{2,i} + m_{3,f} - m_{3,i}}\right)^2 + \left(\frac{\sigma_f}{f}\right)^2}$$

$$C_{<10} = \frac{\left(m_{1,f} - m_{1,i}\right) + \left(m_{2,f} - m_{2,i}\right)}{f_{\text{total,sampling}} \times \dfrac{f_{1,\text{nominal}} + f_{2,\text{nominal}}}{f_{\text{total,nominal}}} \times t_{\text{sampling}}} \times \frac{1000\ \text{mg}}{\text{g}} \times \frac{1000\ \text{L}}{\text{m}^3}$$

$$\sigma_{C,<10} = C_{<10} \times \sqrt{4\left(\frac{\sigma_m}{m_{1,f} - m_{1,i} + m_{2,f} - m_{2,i}}\right)^2 + \left(\frac{\sigma_f}{f}\right)^2}$$

$$C_{<4} = \frac{\left(m_{1,f} - m_{1,i}\right)}{f_{\text{total,sampling}} \times \dfrac{f_{1,\text{nominal}}}{f_{\text{total,nominal}}} \times t_{\text{sampling}}} \times \frac{1000\ \text{mg}}{\text{g}} \times \frac{1000\ \text{L}}{\text{m}^3}$$

$$\sigma_{C,<4} = C_{<4} \times \sqrt{2\left(\frac{\sigma_m}{m_{1,f} - m_{1,i}}\right)^2 + \left(\frac{\sigma_f}{f}\right)^2}$$

Table A–3. Equations for airborne particle concentration and its uncertainty (continued).

$$C_{4-10} = \left[\frac{\left(m_{2,f} - m_{2,i}\right)}{f_{1,\text{nominal}} + f_{2,\text{nominal}}} + \frac{\left(m_{1,f} - m_{1,i}\right)}{f_{1,\text{nominal}} + f_{2,\text{nominal}}} - \frac{\left(m_{1,f} - m_{1,i}\right)}{f_{1,\text{nominal}}} \right] \left[\frac{1000\,\frac{\text{mg}}{\text{g}} \times 1000\,\frac{\text{L}}{\text{m}^3}}{\frac{f_{\text{total,sampling}} \times t_{\text{sampling}}}{f_{\text{total,nominal}}}} \right]$$

$$\sigma_{C,4-10} = C_{4-10} \times \frac{1000\,\frac{\text{mg}}{\text{g}} \times 1000\,\frac{\text{L}}{\text{m}^3}}{\frac{f_{\text{total,sampling}} \times t_{\text{sampling}}}{f_{\text{total,nominal}}}} \times \sqrt{\left\{ \begin{array}{l} \left(\frac{m_{2,f} - m_{2,i}}{f_{1,\text{nominal}} + f_{2,\text{nominal}}} \right)^2 \times \left[2\left(\frac{\sigma_m}{m_{2,f} - m_{2,i}} \right)^2 + \left(\frac{\sigma_f}{f} \right)^2 \right] + \\ \left(\frac{m_{1,f} - m_{1,i}}{f_{1,\text{nominal}} + f_{2,\text{nominal}}} - \frac{m_{1,f} - m_{1,i}}{f_{1,\text{nominal}}} \right)^2 \times \left[2\left(\frac{\sigma_m}{m_{1,f} - m_{1,i}} \right)^2 + \left(\frac{\sigma_f}{f} \right)^2 \right] \end{array} \right\}}$$

$$C_{10-100} = \left[\begin{array}{l} \frac{\left(m_{3,f} - m_{3,i}\right) + \left(m_{2,f} - m_{2,i}\right) + \left(m_{1,f} - m_{1,i}\right)}{f_{1,\text{nominal}} + f_{2,\text{nominal}} + f_{3,\text{nominal}}} \\ - \frac{\left(m_{2,f} - m_{2,i}\right) + \left(m_{1,f} - m_{1,i}\right)}{f_{1,\text{nominal}} + f_{2,\text{nominal}}} \end{array} \right] \left[\frac{1000\,\frac{\text{mg}}{\text{g}} \times 1000\,\frac{\text{L}}{\text{m}^3}}{\left(\frac{f_{\text{total,sampling}} \times t_{\text{sampling}}}{f_{\text{total,nominal}}} \right)} \right]$$

$$\sigma_{C,10-100} = C_{10-100} \times \frac{1000\,\frac{\text{mg}}{\text{g}} \times 1000\,\frac{\text{L}}{\text{m}^3}}{\frac{f_{\text{total,sampling}} \times t_{\text{sampling}}}{f_{\text{total,nominal}}}} \times \sqrt{\left\{ \begin{array}{l} \left(\frac{m_{3,f} - m_{3,i}}{f_{1,\text{nominal}} + f_{2,\text{nominal}} + f_{3,\text{nominal}}} \right)^2 \times \left[2\left(\frac{\sigma_m}{m_{3,f} - m_{3,i}} \right)^2 + \left(\frac{\sigma_f}{f} \right)^2 \right] + \\ \left(\frac{m_{2,f} - m_{2,i}}{f_{1,\text{nominal}} + f_{2,\text{nominal}} + f_{3,\text{nominal}}} - \frac{m_{2,f} - m_{2,i}}{f_{1,\text{nominal}} + f_{2,\text{nominal}}} \right)^2 \times \left[2\left(\frac{\sigma_m}{m_{2,f} - m_{2,i}} \right)^2 + \left(\frac{\sigma_f}{f} \right)^2 \right] + \\ \left(\frac{m_{1,f} - m_{1,i}}{f_{1,\text{nominal}} + f_{2,\text{nominal}} + f_{3,\text{nominal}}} - \frac{m_{1,f} - m_{1,i}}{f_{1,\text{nominal}} + f_{2,\text{nominal}}} \right)^2 \times \left[2\left(\frac{\sigma_m}{m_{1,f} - m_{1,i}} \right)^2 + \left(\frac{\sigma_f}{f} \right)^2 \right] \end{array} \right\}}$$